VERSION 1 OF THE HUBBLE SOURCE CATALOG

Bradley C. Whitmore,[1] Sahar S. Allam,[1,2] Tamás Budavári,[3] Stefano Casertano,[1] Ronald A. Downes,[1]
Thomas Donaldson,[1] S. Michael Fall,[1] Stephen H. Lubow,[1] Lee Quick,[1] Louis-Gregory Strolger,[1]
Geoff Wallace,[1] Richard L. White[1]
Draft version February 17, 2016

ABSTRACT

The Hubble Source Catalog is designed to help optimize science from the *Hubble Space Telescope* by combining the tens of thousands of visit-based source lists in the Hubble Legacy Archive into a single master catalog. Version 1 of the Hubble Source Catalog includes WFPC2, ACS/WFC, WFC3/UVIS, and WFC3/IR photometric data generated using SExtractor software to produce the individual source lists. The catalog includes roughly 80 million detections of 30 million objects involving 112 different detector/filter combinations, and about 160 thousand *HST* exposures. Source lists from Data Release 8 of the Hubble Legacy Archive are matched using an algorithm developed by Budavári & Lubow (2012). The mean photometric accuracy for the catalog as a whole is better than 0.10 mag, with relative accuracy as good as 0.02 mag in certain circumstances (e.g., bright isolated stars). The relative astrometric residuals are typically within 10 mas, with a value for the mode (i.e., most common value) of 2.3 mas. The absolute astrometric accuracy is better than ∼0.1 arcsec for most sources, but can be much larger for a fraction of fields that could not be matched to the PanSTARRS, SDSS, or 2MASS reference systems. In this paper we describe the database design with emphasis on those aspects that enable the users to fully exploit the catalog while avoiding common misunderstandings and potential pitfalls. We provide usage examples to illustrate some of the science capabilities and data quality characteristics, and briefly discuss plans for future improvements to the Hubble Source Catalog.

Subject headings: astrometry – catalogs (HSC) – techniques: photometric – virtual observatory tools

1. INTRODUCTION

The *Hubble Space Telescope* (*HST*) has been in orbit for over 25 years. In that time it has observed with a dozen different instruments, hundreds of observing modes, and roughly a thousand different filters and gratings. Selected, effectively pencil-beam observations have been taken of only a small fraction of the total sky, with a range of exposure times from less than a second (e.g., searches for faint companion planets around very bright stars), to week-long observations of "blank" parts of the sky to observe galaxies at the edge of the universe. This diversity reflects both the promise and the challenge of the Hubble Source Catalog (HSC).

In recent times, computer-based catalogs of astronomical objects have proven to be of great benefit to astronomers (e.g., the Sloan Digital Sky Survey; SDSS, e.g., Ahn et al. 2014). By querying such databases, astronomers are able to carry out research that would otherwise be very time-consuming or completely impractical. Taking a page from this book, the HSC is designed to eventually include the majority of all the objects ever observed by *HST* into a single master catalog. Presently, and primarily due to limitations in the older WFPC2 and ACS source lists which do not go as deep as possible (as discussed in §5), Version 1 contains roughly 20% of the objects it will eventually include. For example, improve-

ments made for Version 2 will increase the size of the HSC by about a factor of three.

Repeat observations are common for *HST*, with 500,000 objects having more than 50 separate observations and 8 million objects observed in more than 10 separate observations. This provides a rich database for variability studies. Regions of the sky with thousands, or even tens of thousands of separate observations (e.g., the Magellanic Clouds—see Figure 1, the Virgo cluster, the Orion Nebula, M31, etc.) can be evaluated in minutes.

The basic scheduling unit for an *HST* observation is a "visit," typically lasting between a single orbit (96 min)
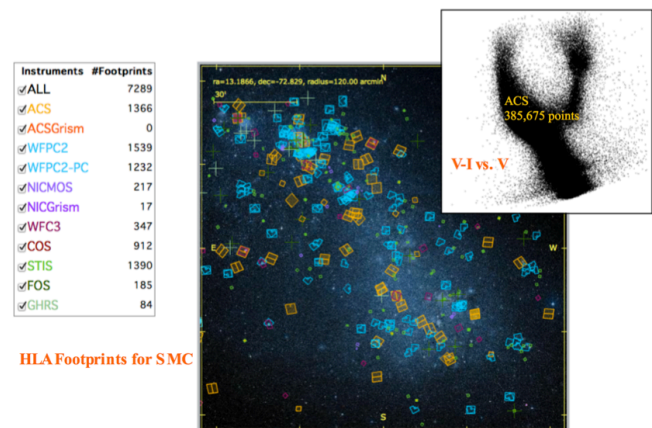
Figure 1. HLA footprints for a search of the SMC using a radius of 2 degrees. A color-magnitude diagram using the ACS-F606W (V) and ACS-F814W (I) filters, containing 385,675 data points, and created by the HSC in less than 2 minutes, is shown in the upper right.

[1] Space Telescope Science Institute (STScI), 3700 San Martin Drive, Baltimore, MD 21218.
[2] Fermi National Accelerator Laboratory, P.O. Box 500, Batavia, IL 60510.
[3] Center for Astrophysical Sciences, Department of Physics and Astronomy, Johns Hopkins University, 3400 North Charles Street, Baltimore, MD 21218.

and six or seven orbits. A visit is also a natural unit for the production of data products from the telescope. For this reason, the Hubble Legacy Archive (HLA, see Jenkner et al. 2006; Whitmore et al. 2008) combines data together in visit-based images and produces source lists for each of these combined images.

In general, an astronomer is not interested in visits, but would like to retrieve all the relevant information for a target observed by *Hubble*. That is the primary driver behind the production of the HSC: to combine the tens of thousands of visit-based HLA source lists into a single master catalog.

The HSC has been available as a Beta (test) version since 2012. Special purpose techniques were developed to handle the challenges of building the HSC. The pipeline, the astrometric and cross-matching algorithms, and the properties of the Beta version of the catalog are described in Budavári & Lubow (2012). In the current paper, we describe Version 1 of the HSC. We provide a brief update on the catalog generation methods and the catalog properties since the original Beta release.

Many astronomical catalogs are produced by telescopes that conduct systematic surveys. The catalog is a key objective of the survey and the observations cover a regular geometric pattern in the sky with uniform properties, such as exposure time and filter set. *The HSC is a very different type of catalog*, as illustrated by Figure 1. Due to the diversity of *Hubble* observations, and accentuated by the fact that the HSC is still in an active developmental stage, the catalog can be very non-uniform, with a patchwork nature in certain regions. This irregularity requires care when developing search criteria. Nevertheless, the HSC is a powerful tool for research with *Hubble* data, even with its limitations, and will be an important reference for future telescopes, such as the *James Webb Space Telescope* (*JWST*), and for survey programs such as PanSTARRS (Panoramic Survey Telescope and Rapid Response System) and LSST (Large Synoptic Survey Telescope).

The HSC is not designed to be all things to all people. The HLA source lists are meant for general-usage rather than being tuned for a particular data set or science requirement. In most cases, a higher science return is possible using a specialized catalog designed for specific needs (e.g., crowded field photometry) or specific science projects (e.g., the Ultra Deep Field). In particular, the High Level Science Products (HLSP; http://archive.stsci.edu/hlsp/) produced by individual science teams are generally of higher quality than the HSC.

The paper is organized as follows. In Section 2 we describe the data used in building Version 1 of the HSC, while in Section 3 we describe the pipeline used to construct the catalog. In Section 4 we examine the photometric and astrometric quality of the HSC. Sections 5 includes advice on avoiding common misunderstandings and potential pitfalls. Section 6 gives a brief summary and describes future plans. The appendices provide comparisons with studies based on use cases, describe tools that can be used to query the HSC, and provide pointers to other relevant information.

2. THE DATA

2.1. *Instruments and Filters*

Version 1 of the HSC includes HLA source lists from the three cameras responsible for the majority of images taken by *Hubble*, namely the Wide Field Planetary Camera 2 (WFPC2), the Wide Field Camera of the Advanced Camera for Surveys (ACS/WFC), and both the ultraviolet/visible and infrared channels of the Wide Field Camera 3 (WFC3/UVIS and WFC3/IR). Source lists from other instruments will be added in the future, including the ACS High Resolution Camera (ACS/HRC) and the Near Infrared Camera and Multi-Object Spectrometer (NICMOS). Data from other cameras (e.g., the imaging modes of the Space Telescope Imaging Spectrograph; STIS) may also be added at a later date.

HSC Version 1 was constructed using HLA Data Release 8 (DR8) images and source lists. These include *HST* data that was public as of 2014 June 1 for WFC3, 2011 February 16 for ACS, and 2009 May 11 for WFPC2. Future releases of the HSC will include more recent data (except for WFPC2, which was removed from *HST* during Servicing Mission 4).

Figure 2 shows the patchwork nature of the *Hubble* observations, with only a small fraction (0.1%) of the full sky being covered. This is a primary difference between the HSC and most other surveys and catalogs. The other major difference is the vast diversity in filter and exposure times at different locations in the sky. Figure 3 is a log-log plot of the number of HSC catalog objects as a function of the number of independent visits to the object by *HST*. The broad distribution is well fit by a power law fit that falls off as the number of visits to the power -2.5.

Table 1 provides some basic parameters and statistics for the different instruments used in the HSC.

Not all images within the Hubble Legacy archive are used by the HSC. About 35% of the combined HLA images (filter-based combined images within a visit) were not included in the HSC for a variety of reasons. For example, the HSC does not include moving target images, images or source lists of low quality, images whose source lists contain less than 10 sources, or images in visits that are likely affected by large numbers of cosmic rays (i.e., exposures of more than 500 seconds with only one exposure taken for the visit).

The majority of the images are from the WFPC2, due to its longevity on *HST* (16 years). An important difference between the WFPC2 and the later generation ACS and WFC3 cameras is the larger WFPC2 pixel size (0.10 arcsec), again highlighting the diversity of *HST* data.

Magnitudes based on observations from different instruments are reported in separate columns of the HSC. For example, all three cameras have an F814W filter, with measurements appearing as the separate columns A_F814W, W2_F814W, and W3_F814W. In most cases users will analyze the data for the different instruments separately, but it is also possible to combine data together. In general this will require the use of photometric transformation equations and aperture corrections. This is discussed further in Section 4.1.3.
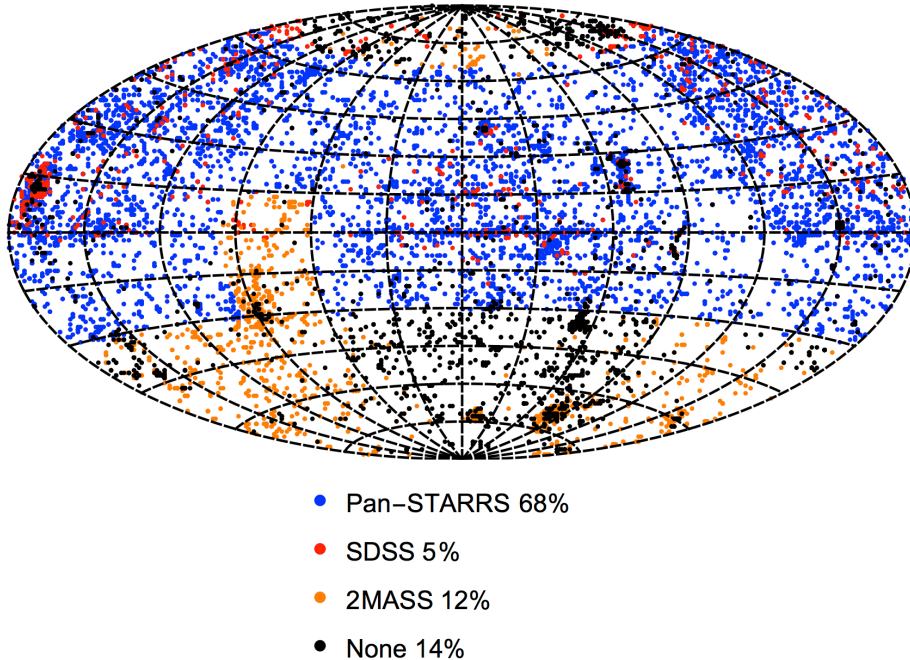
Figure 2. Piecemeal sky coverage showing HLA images used to build the HSC. Color coding shows where PanSTARRS (pre-release version—PV1—e.g., see Stubbs et al. 2010), SDSS (Ahn et al. 2014), and 2MASS (Skrutskie et al. 2006) are used to provide the astrometric backbone for the HSC.

Table 1
Basic HSC Statistics

Instrument	# Filters	# Images[a]	# Detections[b]	Area[c] (sq deg)	Pixel Size (arcsec)	Aperture sizes[d] (arcsec)
(1)	(2)	(3)	(4)	(5)	(6)	(7)
WFPC2	38	29,146	13×10^6	30	0.10	0.10, 0.30
ACS/WFC	12	9,021	21×10^6	21	0.05	0.05, 0.15
WFC3/UVIS	47	4,772	31×10^6	5	0.04	0.05, 0.15
WFC3/IR	15	6,763	14×10^6	5	0.09	0.15, 0.45
Total	112	49,702	79×10^6	61	$\cdots$	$\cdots$

[a] Number of images contributing source measurements.
[b] Total number of source detections from all filters.
[c] Sum of the areas of visit-level combined images. This estimate ignores overlaps of these images.
[d] Radii of the two circular apertures used for aperture photometry.

3. THE CATALOG

The SExtractor software (Bertin & Arnouts 1996) is used to produce the HLA source lists used in the HSC. Both aperture magnitudes (`MagAper1` and `MagAper2`: see Table 1; note that these are not total magnitudes since no aperture corrections have been made to these values), and total magnitudes (using the `MagAuto` algorithm in SExtractor to attempt to include all the light in the source) are provided in the HSC. The ABMAG system is used for the HSC; transformations are required to convert to other systems such as VEGAMAG or STMAG. DAOPHOT (Stetson 1987) source lists are also produced in the HLA, primarily for point sources. These are not used in the HSC however.

The radius used for the small and large aperture measurements (`MagAper1` and `MagAper2`) are 1 and 3 pixels for WFPC2 and ACS; 1.25 and 3.75 pixels for WFC3/UVIS; and 1.67 and 5 pixels for WFC3/IR. See Table 1 for the corresponding sizes in arcsec. The sky

background is defined as the median in an annulus from 5 to 10 pixels. In most cases, the detection threshold is set to three times the background noise, although it is adjusted in some regions in accordance with the source flagging (e.g., around very bright stars).

Unlike ACS and WFC3, WFPC2 source lists explicitly include a correction for Charge Transfer Efficiency (CTE) loss, based on the formulae from Dolphin (2009). Images with pixel-to-pixel corrections using the algorithm developed by Anderson & Bedin (2010) will be used to construct ACS and WFC3 source lists in the future.

3.1. How the Catalog is Constructed

The HLA source lists provide the starting point for the HSC construction. These lists provide the characteristics of sources that are contained in visit-based *HST* images. The HSC construction involves cross-matching the sources in these source lists. In broad outline, the relative astrometry of overlapping images is improved from the
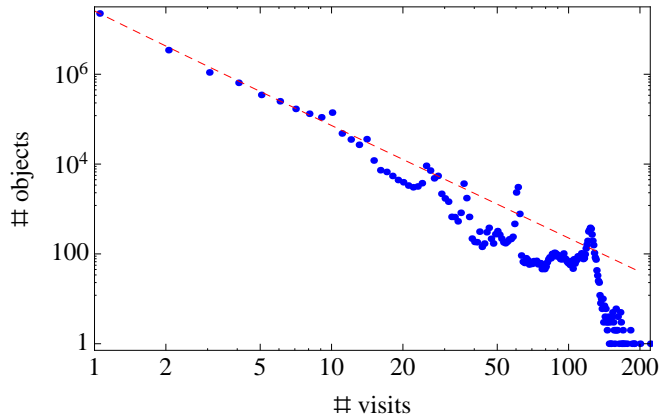
Figure 3. The number of objects (matches) in the HSC catalog as a function of the number of visits in each match. The dashed line is a power law fit that falls off as the number of visits to the power -2.5. Peaks in the distribution are partially due to repeat observations of: the Galactic bulge ($\sim$25 visits), M31 Halo ($\sim$60 visits), and M4 ($\sim$120 visits).

currently available HLA astrometry. Next, the sources that are in the overlapping images are cross identified on the basis of source position. Aspects of the reduction pipeline, the astrometric and cross-matching algorithms, and the properties of the Beta version catalog, are described in Budavári & Lubow (2012). See also Budavári & Szalay (2008) for a discussion of the Bayesian approach at the heart of the cross-matching step, Lubow & Budavári (2013) for more details about the cross-matching algorithm, and Whitmore et al. (2008) for details about the early source list generation.

The basic steps involved in the construction of the HLA source lists, and the subsequent construction of Version 1 of the HSC, are briefly described below. More detailed descriptions of various aspects of the process are available in the references provided above, or in the HLA and HSC Frequently Asked Questions (FAQs; see Appendix D).

1. Within the HLA, combine exposures for each filter within a visit using `multidrizzle` (Fruchter 2009) for WFPC2 and ACS, and using `astrodrizzle` (http://drizzlepac.stsci.edu/) for WFC3. The background is subtracted for the WFPC2 and ACS, but not for the WFC3 images. Inclusion of the background allows the source-finding parameters to be set to find fainter sources for the WFC3. In addition, a different spatial filter technique is used for sparse (Gaussian) and crowded (Mexican hat) fields in the WFC3 images (see http://hla.stsci.edu/hla_faq.html#Source6 for a more detailed discussion). New WFPC2 and ACS images will be made for the HLA using the approach used for the WFC3 in the future. For the current WFPC2 and ACS images, but not for the current WFC3 images, a comparison is made with the SDSS and GSC2 catalogs to improve the absolute astrometric positions of the HLA source lists at this stage. Additional astrometric adjustments are made at various other steps, as described below.

2. Combine the filter-based images into a "white-light" image (i.e., combine data from different fil-

ters, but within the same visit, to provide a deeper image with a wider wavelength range). A white-light image serves as the detection image for the visit. No shifts are made to align WFPC2 and ACS exposures within a visit before combining the data. For WFC3, an early version of the `tweakreg` algorithm within the `astrodrizzle` software package was used to align the sub-images within a visit, prior to combining the images for the different filters.

3. Run SExtractor on the white-light (detection) images to obtain white-light source lists. The filter-based source characteristics are then determined at each of the detection-based source positions. If no source is detected for a particular filter at the source position, then that information is maintained as a filter-based nondetection. Nondetections are listed in the HSC Detailed Catalog (i.e., as "N" in the Det column), which is discussed in point 8 below. While both SExtractor and DAOPHOT source lists are available in the HLA, only the SExtractor source lists are used in the HSC. However, a comparison is made between various aspects of the DAOPHOT and SExtractor source lists at this stage to help weed out bad images and bad source lists before including them in the HSC database. Appendix C shows examples of the parameter files used to produce the SExtractor and DAOPHOT source lists, in this case for WFPC2.

Two different magnitudes are included in the HSC: `MagAper2` (aperture magnitudes—see Table 1 for sizes on the sky) and `MagAuto` (SExtractor estimates of the total magnitude primarily designed for extended sources). Smaller aperture measurements (`MagAper1`) can be recovered via the Concentration Index (CI), which is the difference between `MagAper1` and `MagAper2`. Source properties such as the CI and the distance to nearby bright stars are also used to determine whether a source is likely to be an artifact. Such false detections are not included in the HSC. The complete set of attributes measured by SExtractor is accessible through links from the HSC back to the original HLA source lists.

4. Apply astrometric "pre-offsets" based on cross matching with three reference catalogs: PanSTARRS, SDSS, and 2MASS. This is needed, for example, to reduce the typical $\sim$1–2 arcsec absolute astrometric errors for *HST* images before Guide Star Catalog 2 became available in late 2005, to less than 0.3 arcsec. This step determines the statistical mode of the binned astrometric offsets between the *HST* sources and those in a reference catalog. The method is very robust to large offsets and has a precision of a few tenths of an arcsec. Although this astrometric accuracy is not adeqaute for cross matching sources in different *HST* images, it is sufficient for permitting convergence of the high accuracy Budavári and Lubow (2012) relative astrometry determination. Without the pre-offsets, the number of false matches across *HST* source lists in very
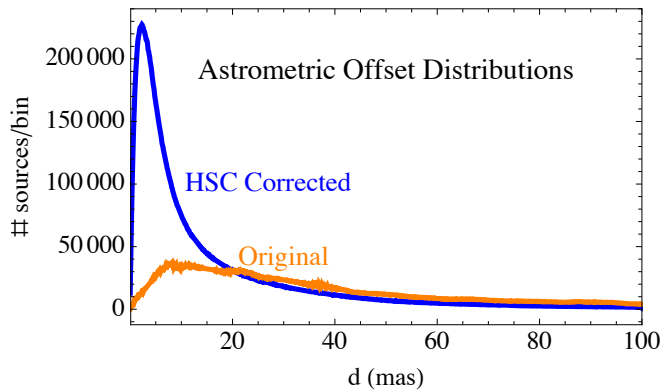
Figure 4. Distribution of astrometric residuals before and after the Budavári & Lubow (2012) algorithms are employed. The areas under the two curves are the same, but the residual distribution before corrections has a very long tail that extends to much larger values. The mode (peak) for the corrected curve is 2.3 mas.

crowded fields (e.g., globular clusters) prevents the Budavári and Lubow (2012) relative astrometry correction algorithm from converging in many cases.

5. Separate the white-light images into groups of overlapping images. Within each image group, determine the relative shifts (and rotations) needed to align the various images (see the Budavári & Lubow 2012 paper for details on these two operations). This reduces the relative astrometric accuracy from a few tenths of an arcsec to less than 10 mas in most cases (see Figure 4 and the discussion in Section 4.2). Apply these image shifts to the sources in each white-light source list.

6. Cross-match the white-light sources by position. This is initially done using a friends-of-friends (FoF) algorithm with a specified search radius. FoF cross-matching can result in long chains of loosely connected sources that should be further split. Various ways of splitting each FoF match are considered by the software to determine the best partitioning. Estimates of the astrometric uncertainties and the quality of a particular partioning for a match are determined by computing a Bayes factor using the formalism described in Budavári & Szalay (2008). We apply a greedy algorithm that reduces the number of partitions examined, as described in Budavári & Lubow (2012). In most matches, the initial FoF match is found to have the best Bayes factor, and so no splitting is done.

7. Readjust the absolute astrometry for each group using PanSTARRS, SDSS, or 2MASS as the reference. The absolute astrometric accuracy for the three reference catalogs is approximately 0.1 arcsec (e.g., see Pier et al. 2003 for SDSS and Skrutskie et al. 2006 for 2MASS; PanSTARRS uses SDSS as its astrometric backbone so should have similar accuracy). Hence the typical absolute astrometric accuracy for the HSC should be about 0.1 arcsec (but see Section 4.2.3 for results that show it may be somewhat better in some cases).

Figure 2 shows that in 14% of the images, involving 32% of the visits, there are insufficient matches

with PanSTARRS, SDSS, or 2MASS to allow a correction. Most commonly this happens because both SDSS and PanSTARRS have limited sky coverage and 2MASS sources are sparse in the extragalactic sky. There are other reasons why absolute astrometric corrections cannot be made for parts of the HSC, for example for many far UV images when there are no objects in common with the three reference catalogs. Another reason that there may be no absolute correction is that singleton images (images that do not overlap with other images—about 20%) did not get corrected by the post-processing step in version 1. That will be corrected in future versions of the HSC. In the end, 80% of the HSC matches have the Absolute Correction (`AbsCorr`) flag set to yes (Y).

8. Using the white-light source lists with corrected astrometry, the cross-matched white-light sources, and the filter-based source lists, build the HSC Detailed Catalog, which includes visit- and filter-based information about each source. Also, build the HSC Summary Catalog. This contains the aggregate properties for each set of cross-matched sources, such as the mean position, the mean magnitudes and their standard deviations. It also includes some useful ancillary data such as the galactic extinction (i.e., $E(B–V)$ values from Schlegel 1998) at that position on the sky.

Steps 1 through 3 above use the HLA image and source list processing, while steps 4 through 8 are carried out in a Microsoft SQL Server database. The catalogs are made available though a set of database tables that can be accessed by various user interfaces, as will be discussed in §5. In addition, there are database stored procedures and functions that use special indexes and algorithms to provide rapid access to HSC information. This makes it possible for users to make complex requests through the user interfaces, such as cross matching HSC against a user-supplied set of positions, with fast response times. Currently, the Discovery Portal, the Hubble Legacy Archive image display, and the MAST (Mikulski Archive for Space Telescopes) search forms access the HSC database using these stored procedures and functions. In addition, the CasJobs interface allows users to directly access the functions and run more general SQL queries. See Appendix B for more information about these four interfaces.

4. QUALITY ASSESSMENT

A three-pronged approach is used to characterize the quality of the HSC. We first examine a few specific datasets, comparing magnitudes and positions directly for repeat measurements. The comparisons are first made using the same instrument and filter, and then made using different instruments and filters.

The second approach is to compare repeat measurements for the full database. While this provides a better representation of the entire dataset, it can also be misleading since the tails of the distributions are generally caused by a small number of bad images, bad source lists, and other artifacts.

The third approach is to produce a few well-known astronomical figures (e.g., color-magnitude diagram for

the outer disk of M31from Brown et al. 2009) based on HSC data, and compare them with the original study. Three examples of this third approach are provided in Appendix A.

This three-pronged approach is hierarchal in nature: 1) a spot check on the consistency and quality of the source lists for a few specific data sets, 2) a check that the entire dataset is relatively homogenous and of high quality, and 3) a check that we are consistent with completely independent datasets or independent analysis techniques.

As stressed in other parts of this paper (e.g., Section 5, "Caveats and Warnings"), it is important to keep in mind that parts of the HSC can be very non-uniform. Hence, researchers cannot assume that the results reported in this section represent the entire database. If uniformity is important for a specific science project, a careful examination of the data is required, including viewing the images themselves. In many cases it is possible to filter the HSC data and improve the uniformity of the data. This topic will be discussed in Section 4.1.4.

4.1. Photometric Spot Checks

4.1.1. Point Source Photometry—Single Instrument/Filter Checks

Since we are primarily interested in stellar photometry in this section, aperture magnitudes (i.e., `MagAper2`) are used throughout.

Our first photometry check examines the Brown et al. (2009) deep ACS/WFC observations of the outer disk of M31 using objects within 2.5 arcmin of the J2000 search position $00^{\rm h}49^{\rm m}08.09^{\rm s}$ $+42°44'55.0''$. The observing plan for this proposal (ID = 10265) resulted in approximately 60 separate one-orbit visits (not typical of most *HST* observations), hence providing an excellent opportunity for determining the true uncertainties by examining repeat measurements.

Figure 5 shows a small part of the field with the HSC overlaid. Only sources detected on more than five images (`NumImages` > 5) are included in order to filter out cosmic rays. Note that relatively faint stars are not included; the more recent WFC3 HLA sources lists (and future ACS and WFPC2 source lists) are more aggressive in this regard. The completeness limits for the HSC when compared to the Brown et al. (2009) catalog are roughly 95% in the F606W and F814W filters out to about 26th magnitude.

Figure 6 shows that the photometric agreement between the HSC and Brown et al. catalog is quite good, with zeropoint differences of only a few hundredths of a magnitude after corrections from ABMAG to STMAG and from aperture to total magnitudes are made. The photometric scatter is about 0.04 mag in general, and better than 0.02 mag for the brighter stars. The zero point offsets between the HSC and the Brown et al. catalog are likely to be due mainly to the inclusion of a CTE (Charge Transfer Efficiency) correction by Brown et al., but not by the HSC in Version 1. The sense of the difference is in the right direction, with the HSC magnitudes slightly fainter, and the magnitude of the offset is also reasonable, since Brown et al. (2006) comment that the expected CTE corrections are a "few hundredths of a magnitude" in fields like these. More details are available in HSC Use Case #1 (see Appendix A.1).
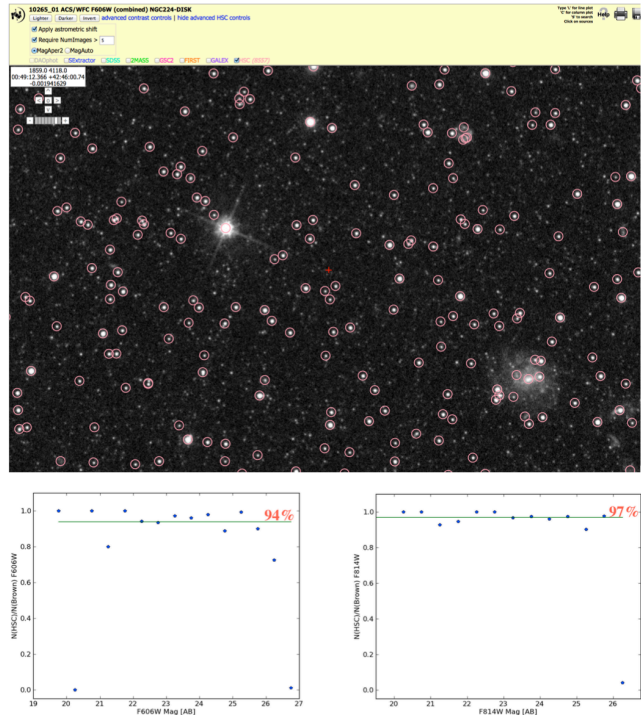
Figure 5. Example of the quality of the HSC in the outer disk of M31overlaid on an ACS image from proposal 10265. The bottom plots show the completeness levels for the F606W and F814W observations when compared to the Brown et al. (2009) study.
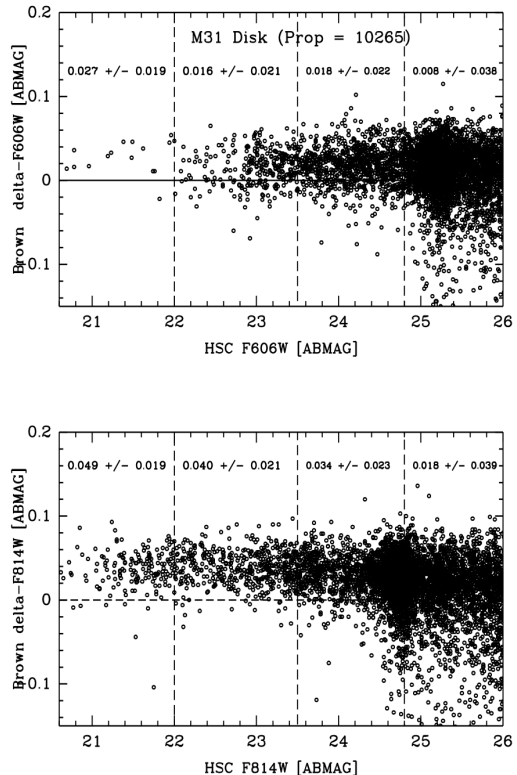
Figure 6. Comparison of HSC and Brown et al. (2009) photometry, with means and RMS scatter listed for four magnitude ranges. The top (bottom) panel shows the F606W (F814W) magnitude difference; objects are systematically slightly fainter in the HSC.

The use of short, one-orbit visits in proposal 10265 leads to one of the common limitations of the HSC, namely brighter completeness limit for HLA source lists than are possible by combining all the data. For example, the deep, co-added, 30 orbit for each filter image used by Brown et al. goes roughly four magnitudes deeper than the HSC, as will be shown in §4.4.1.

A more representative comparison would be with catalogs produced using one-orbit visits. These cover a wide range of quality and completeness limits depending on the specific science requirements. Typical studies reach roughly the same level as the WFC3 source lists in the HSC while state-of-art studies like the Panchromatic Hubble Andromeda Treasury program (PHAT; e.g., see Williams et al. 2014) go roughly two magnitudes deeper in the confusion-limited IR images. A detailed comparison between the HSC and PHAT will be provides as a use case for the Version 2 HSC release, currently planned for spring of 2016.

4.1.2. *Point Source Photometry—Error Estimates*

Figure 7 shows a comparison between estimated photometric errors based on SExtractor measurements (i.e., magerr), and the true scatter based on repeat measurements (i.e., values of sigma reported in the HSC summary catalog). We find that the quoted values of magerr are roughly a factor of three too low for WFPC2 and ACS observations, but are in relatively good agreement for the newer WFC3 source lists.

We also note that the sigma estimates increase rather dramatically at bright magnitudes for WFPC2, and to a lesser degree for ACS as well. This is due to the inclusion of a few saturated stars that have made it through the filtering designed to flag and remove them (see the discussion in §4.1.4). These problems will be rectified in the near future when the pipeline developed for the newer WFC3 source lists is used to produce the next generation of WFPC2 and ACS HLA source lists.

### 4.1.3. *Point Source Photometry—Cross-Instrument/Filter Checks*

The globular cluster M4 (using a search within $200''$ of $16^h23^m38.66^s\ -26°32'10.9''$) provides a good opportunity to compare the HSC photometric system for all three instruments. Figure 8 shows comparisons in the "V" filters (i.e., WFPC2-F555W, ACS-F606W, and WFC3-F547M) and "I" filters (i.e., WFPC2-F814W, ACS-F814W, and WFC3-F814W).

Starting with the best case, ACS-F814W vs. WFC3-F814W shows excellent results, with a slope near unity, values of RMS around 0.04 magnitudes, and essentially no outliers. The good agreement also suggests that ACS-F814W and WFC3-F814W measurements can be added together with little loss of photometric accuracy. This is not true, as we will see below, when the filter bandpasses are not as similar. In general, photometric transformations are necessary before combing observations using different instruments.

An examination of the WFPC2-F814W vs. WFC3-F814W and ACS-F814W vs. WFPC2-F814W comparisons show that there is an issue with the WFPC2 data. The short curved lines deviating from the one-to-one relationship show evidence of the inclusion of a small number of slightly saturated measurements for bright stars
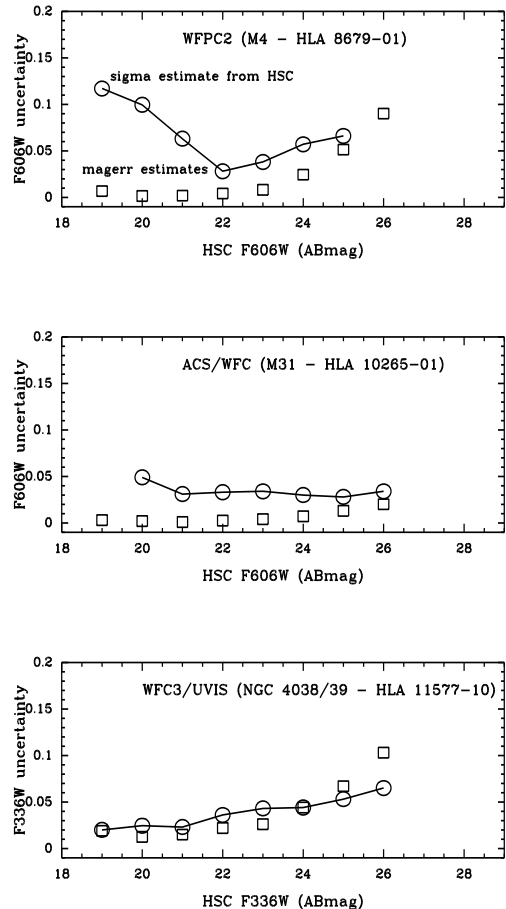

Figure 7. Comparison of HSC sigma values (i.e., RMS scatter based on repeat measurements [circles] with magerr estimates based on SExtractor squares). The upturn in the sigma estimate for the WFPC2 at bright magnitudes is due to inadequate filtering of a few saturated stars, as discussed in the text.
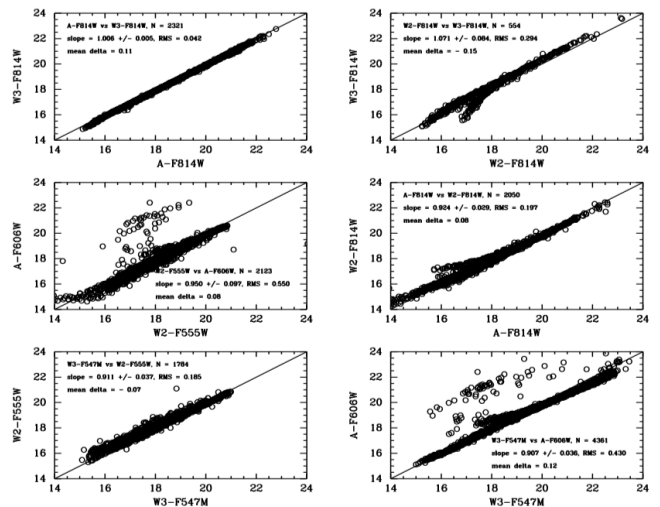

Figure 8. Comparisons of repeat measurements for similar filters in the globular cluster M4. Note that photometric transformations between the instrument/filter combinations would be required before the different observations could be combined, if desired.

(i.e., roughly 5% of the data), as already mentioned in the discussion of Figure 7.

There is a similar but smaller issue with the ACS data,
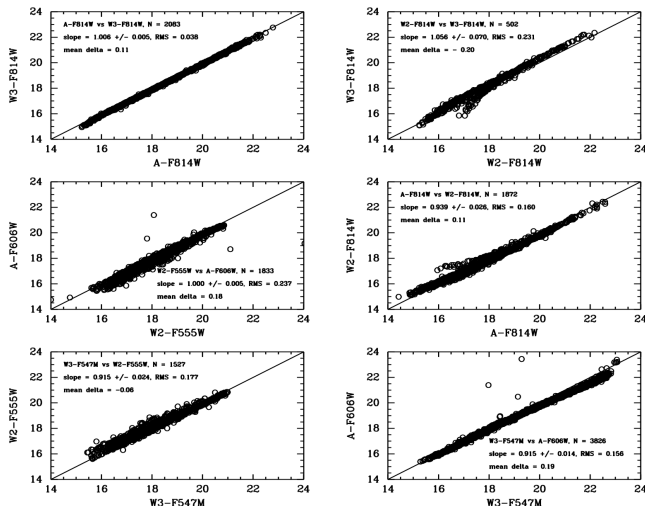
Figure 9. Same as Figure 8, but with the four constraints discussed in Section 4.1.4 imposed.
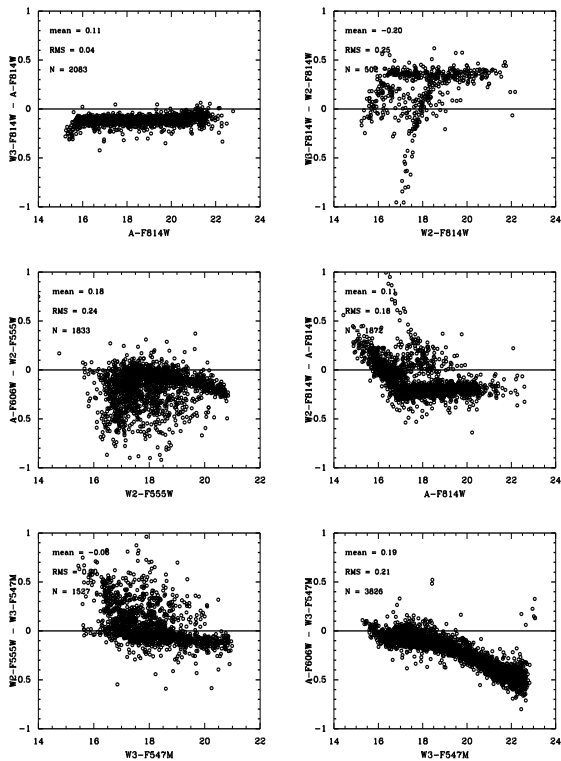
Figure 10. Same as Figure 9, but with residuals rather than a one-to-one plot to show the small-scale features.

as shown by the WFC3-F547M vs. ACS-F606W comparison.

Much larger deviations are also seen in the two panels making use of ACS-F606W observations, where a cloud of outliers is found several magnitudes off the one-to-one line. These are caused by combining data from short (20 sec) and long (1800 sec) sub exposures. These issues will be fixed in future versions of the HSC, but it is also relatively easy to filter them out, as discussed in §4.1.4.

A careful look at Figure 8 also shows systematic devi-

ations in the slope of the relationships, with deviations of a few tenths of a magnitude at the extremes (e.g., WFC3-F547M vs. ACS-F606W). Figure 10 in §4.1.4 shows this more clearly. These are examples where the filters are not well matched (e.g., the central wavelength and width are 591.8 and 158.3 nm for the ACS-F606W filter but 544.7 and 65.0 nm for the WFC3-F547M filter). Hence sources with different colors (and hence different brightnesses since this is a globular cluster with a well-defined main sequence) deviate in the two filters. A photometric transformation would need to be made before photometry in these two filters could be combined. The comparison is made here in order to evaluate the RMS scatter, not to imply that the data from different instruments/filters can be added together without the loss of a few tenths of a magnitude in accuracy.

Other complications that can cause deviations are issues having to do with Charge Transfer Efficiency (CTE) loss (i.e., for WFPC2 a correction is made using the Dolphin 2009 formula, but no corrections are made for ACS and WFC3 in Version 1), differences in aperture corrections (typical differences between the different instruments are about 0.1 mag for the ACS, WFC3/UVIS, and WFPC2), and differences in exposure times (e.g., resulting in different completeness limits and signal-to-noise ratios—see the transition at about the 19th magnitude in the WFPC2-F555W vs. ACS-F606W diagram with larger scatter at brighter rather than fainter magnitudes).

4.1.4. Filtering out Artifacts

As stressed throughout this paper, the diverse nature of the *HST* archival database can result in a number of artifacts. However, we also note that the availability of multiple observations in many cases provides the opportunity to identify artifacts and filter them out, a circumstance that is not always possible with more limited datasets where similar artifacts may still be present but go undetected.

Figure 9 shows the same comparisons as Figure 8, but with four constraints included. These are:

- NumImages > 2 (to remove residual cosmic rays),
- CI < 1.4 (to remove extended sources and blends),
- CI_Sigma < 0.5 (to remove partially saturated stars), and
- *filter*_Sigma < 0.2 (to remove low S/N data and saturated stars),

where CI is the Concentration Index (i.e., the difference between the small and large aperture magnitudes—see Table 1), and CI_Sigma and *filter*_Sigma refer to the RMS scatter among repeat measurements of the CI value and the magnitude in a given filter.

As shown in Figure 9, the number of artifacts and discrepant points is greatly reduced, with only 3/3826 (0.1%) artifacts remaining in the WFC3-F547M vs. ACS-F606W comparison with residuals greater than 1 mag. The values of RMS scatter from the line are also reduced, in some cases by more than a factor of two. The values of "true RMS" shown in Figure 9, which are the values after the remaining outliers have been removed, range from 0.04 to 0.17 magnitudes.
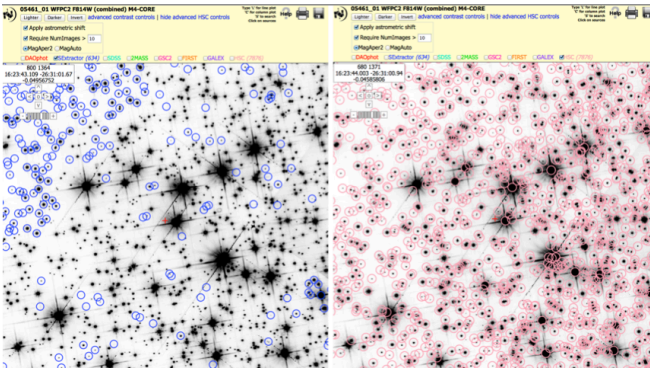
Figure 11. The left image shows a WFPC2 SExtractor source list (blue) in the globular cluster M4. Note how nonuniform the coverage is with missing sources where the background is high. The right image shows the more uniform HSC coverage (pink circles). It is more uniform due to the presence of WFC3 source lists in this field. See discussion in §4.1.3 for more details.

Figure 10 shows a version of Figure 9 with residuals rather than a one-to-one plot. This allows us to see the small-scale features more clearly, especially the slight curvatures due to the mismatch in filters (e.g., the bottom right panel) and the increase in scatter for shorter exposures (e.g., the two bottom left panels), as discussed in §4.1.3 . These figures also show the inherent danger of combining data from different instruments and filters. Although this might be appropriate in certain cases (e.g., the upper left panel), it should only be attempted with great care.

While the specific criteria may change for different datasets and scientific purposes, some combination of the four artifact filters employed in this section can often be used to improve the photometry from the HSC.

Another form of "artifact" is the non-uniformity inherent in a dataset as diverse as the *Hubble* archives. This is accentuated by the current poorer quality of the WFPC2 and ACS HLA source lists relative to the more recently generated WFC3 source lists. For example, Figure 11 shows that many sources are missed in regions with high background in this WFPC2 image. SExtractor tends to combine high background regions into larger "extended" objects, missing obvious stars in cases like Figure 11. While SExtractor parameters can be tuned to largely alleviate this problem for a specific image, this is difficult for the HLA due to the diversity of the images. As discussed in the first bullet in §3.1, a Mexican hat kernel is now used in the HLA for WFC3 images in crowded regions, largely eliminating this problem. The same algorithm will be used for WFPC2 and ACS in the future.

While the overall coverage of the HSC is quite good (i.e., the pink circles in Figure 11), thanks mainly to the WFC3 images in this region, users should keep in mind that just because a given observation is missing in the HSC does not mean that it has not been observed by *Hubble*.

More details about the comparisons discussed above, as well as other examples relevant to photometric accuracy, can be found in HSC Use Case #1 (Stellar Photometry in M31), HSC Use Case #2 (Globular Clusters in M87 and a Color Magnitude Diagram for the LMC), and HSC Use Case #5 (White Dwarfs in the Globular Cluster M4). See Appendix D for URLs for these and other HSC use
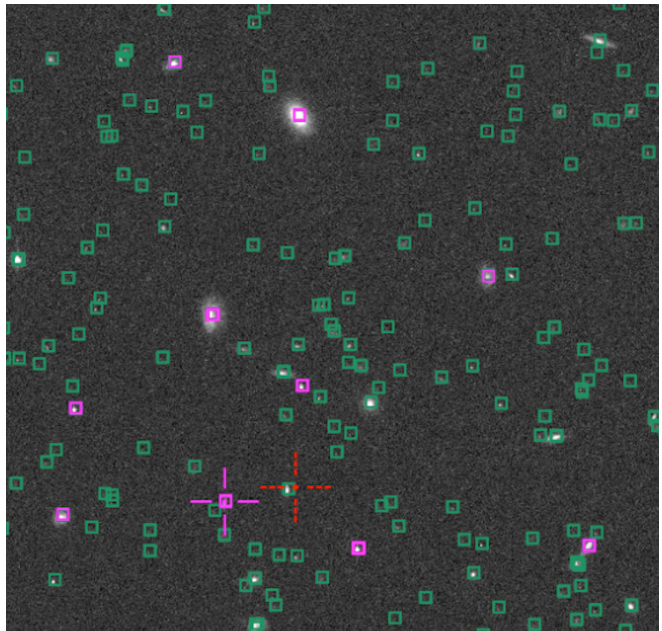
Figure 12. Comparison of HSC (green) and SDSS (pink) in a small part of the Hubble Deep Field. This shows the increased depth using the HSC (approximately 150 objects) compared to the SDSS (9 objects). The image was made using the MAST Discovery Portal with an *HST* image as the background.

cases.

4.1.5. *Extended Object Photometry—SDSS Observations in the Hubble Deep Field*

In this section we make photometric comparisons with extended targets, such as distant galaxies. Hence, values obtained using the Source Extractor algorithm `MagAuto` are used to estimate the total magnitudes rather than the aperture magnitudes (`MagAper2`) used in the previous sections.

The Sloan Digital Sky Survey (SDSS) has been tremendously successful, due to both the high quality, wide-field, uniform database, and to the extensive extraction and analysis tools it has made available to researchers. It has taken the field of "database astronomy" to a new level, and in many ways is the inspiration for the HSC.

A comparison between the HSC and SDSS provides an opportunity for highlighting both the similarities (e.g., agreement between photometric results; availability of CasJobs) and differences (e.g., the HSC goes deeper but with "pencil beam" coverage; the HSC can be very non-uniform in certain regions).

Figure 12 shows the overlap between the HSC and SDSS coverage in a small part of the Hubble Deep Field (HDF). There are 9 objects in common out of the roughly 150 HSC sources in this field. The SDSS (using DR12; Alam et al. 2015) has a completeness limit around $r = 22.5$ mag while the HSC goes to ACS-F775W = 26.0 mag.

Figure 13 shows the photometric comparisons between the HSC and SDSS for a wide variety of filters. We find reasonably good agreement. Both the scatter and the offsets are typically a several tenths of a magnitude. The offsets primarily arise from differences in photometric filters and bandpass, since no transformations have been made for these comparisons.

The best agreement is between WFPC2-F814W and
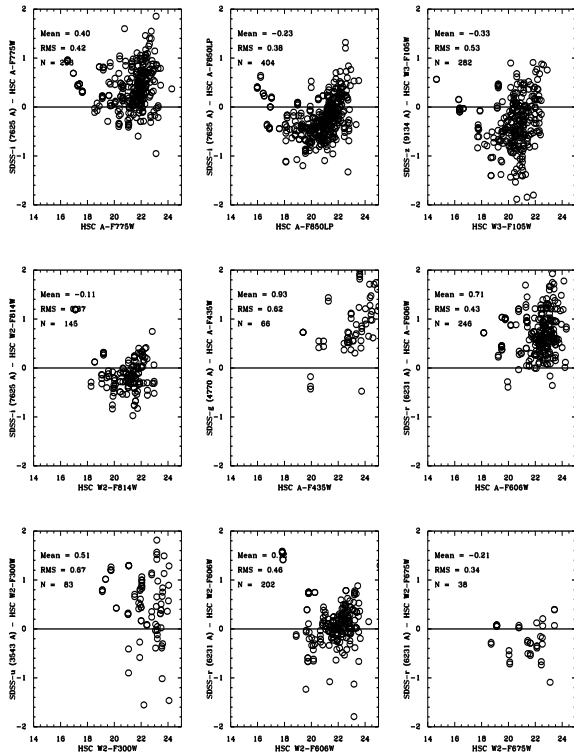
Figure 13. Comparison between HSC photometry (`MagAuto`) and SDSS (DR12, Alam et al. 2015; psfMag values) photometry for the Hubble Deep Field (i.e., RA = 189.206, DEC = 62.2161, r = 500 arcsec). Note that photometric transformations between the instrument/filter combinations would be required before the different observations could be combined, if desired.

SDSS-i, with a mean offset of -0.11 and a RMS scatter of 0.37 mag. The mean photometric scatter for repeat HSC measurements in the ACS-F850LP filter is about 0.10 mag while for the SDSS-i the scatter is about 0.15 mag. In quadrature these add to 0.18 mag, explaining some but not all of the observed scatter in the comparison. Differences between SExtractor parameters (e.g., thresholds, filtering algorithms, and deblending values) in the HSC and SDSS are responsible for most of the rest of the difference.

The relatively small scatter for this particular comparison reflects the fact that these two filters are very similar, hence the transformation is nearly one-to-one. This is not true for many of the other comparisons in Figure 13.

Figures 12 and 13 used `NumImages` > 10, and a value for the cross-match radius of 0.2 arcsec. Care must be taken to choose optimal values for these parameters to filter out artifacts and mismatches between sources. Even so, some manual weeding is often necessary. In this particular case the objects are isolated enough to make this a minor issue, with only a few mismatches present (i.e., the outliers in the SDSS-r vs. HSC ACS-F606W comparison).

4.2. *Astrometric Spot Checks*

The quality of point source astrometry for the HSC can vary for reasons similar to those relevant to photometric
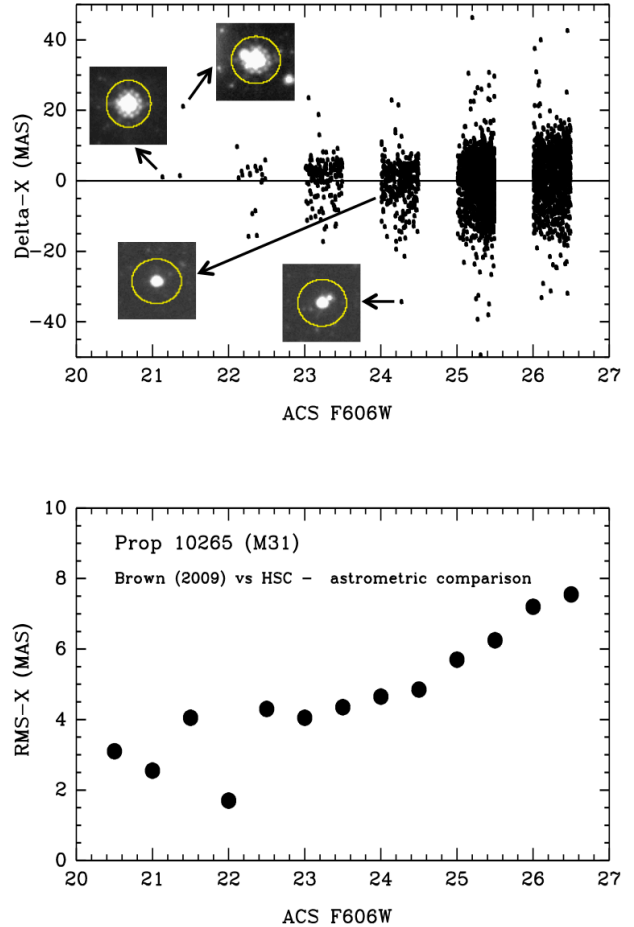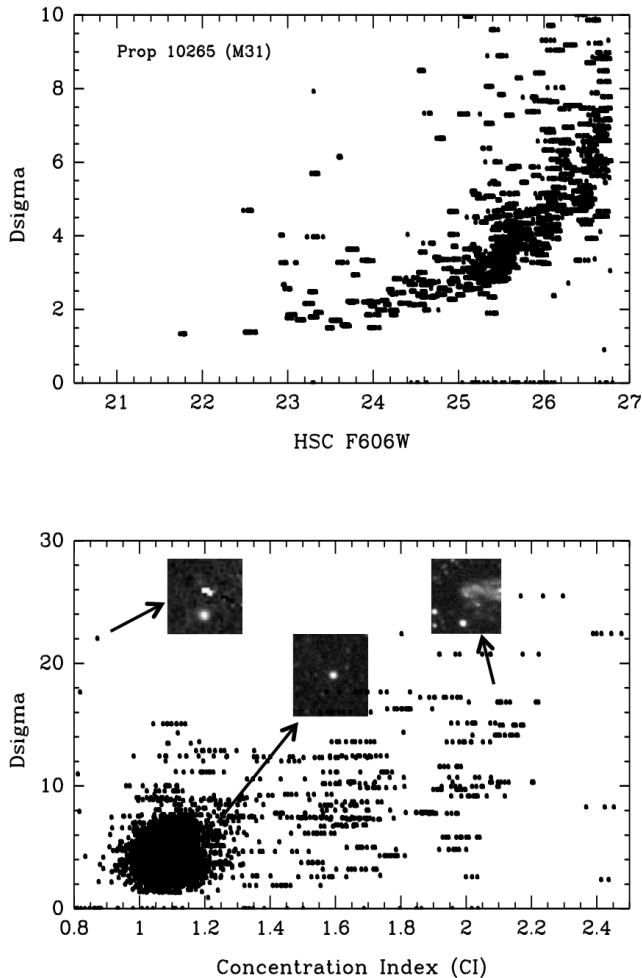

Figure 14. Comparison of positions (in the X direction) between the HSC and the Brown et al. (2009) HLSP catalog. The top panel shows comparisons for each object while the bottom panel shows the RMS scatter in repeat measurements as a function of magnitude.

measurements. These include non-uniformities due to the wide range of instruments, different exposures times, and different observing strategies used by the observers. In this section we use the same approach as employed for photometry, starting with comparisons using a single instrument, then comparing different instruments, and latter making comparisons for the entire database.

4.2.1. *Relative Point Source Astrometry—Single Instrument (ACS/WFC)*

We begin with the same dataset used in §4.1.1, namely the Brown et al. (2009) ACS/WFC observations in the outer disk of M31 (prop ID = 10265; see HSC Use Case #1, and for more details, Archival HSC Use Case #1). Figure 14 shows position comparisons in the X-direction (using the 10265-01-ACS/WFC-F606W HLA image as the reference) between values from the High Level Science Products (HLSP) catalog provided by Brown et al., and the measurements from the HSC. There are several differences in these treatments, perhaps the most basic being that Brown et al. combined the 30 different visits for each filter into a single deep mosaic image, while the HSC makes 30 separate source lists and then combines the results, as described in §4.1.1.
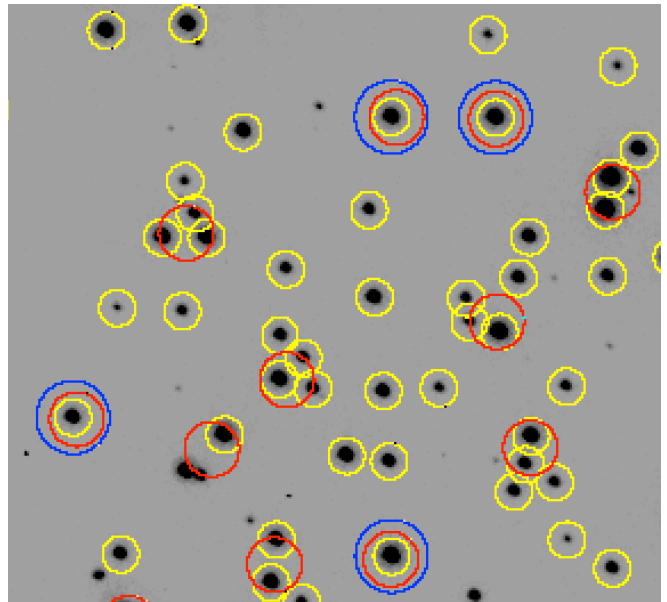
The upper panel of Figure 14 shows the resulting com-

Figure 15. Comparisons between Dsigma (in mas), ACS-F606W magnitudes from the HSC (top), and Concentration Index (bottom) in the Brown et al. (2009) M31 disk field. See text for description.

Figure 16. Comparison of HSC (yellow) and PanSTARRS (red) astrometry in M4. Blue circles show an example of the matches used to measure a mean relative astrometric shift of approximately 9 mas between the HSC and PanSTARRS for this field, after filtering out poor matches due to differences in spatial resolution. See text for details.

(as shown in the cutout for one object) or blended stars where the centroiding is less precise. The vast majority of objects are isolated stars with values of CI around 1.1 and Dsigma between 2 and 8 mas. A few rare artifacts are also found with discrepant values such as the detector defect shown in the cutout in the upper left of the right figure.

A general conclusion based on both Figure 14 and 15 is that the limiting values for the astrometric precisions for a single well exposed ACS or WFC3 observations in the HSC is a few mas. This agrees with results we will find using full database comparisons in §4.3.2. Astrometric positions for WFPC2 are considerably more uncertain due to a variety of considerations including larger pixels and more uncertain geometric solutions, especially for objects that fall on both the PC and WFC chips in subsequent exposures. This topic will be discussed in more detail in §4.3.

4.2.2. *Absolute Astrometry for Point Sources*

As discussed in §3.1 and shown in Figure 2, three different datasets have been used to provide the astrometric backbone for the HSC, with PanSTARRS being used in the majority of the cases. Hence, we expect the typical accuracy for the absolute astrometry of the HSC to be roughly the same as for PanSTARRS. PanSTARRS uses the 2MASS catalog as its astrometric backbone, and so should have roughly the same 0.1 arcsec (i.e., 100 mas) absolute astronomical accuracy (Skutskie et al. 2006). In this section we perform independent spot checks to make sure the HSC fields are well aligned with the PanSTARRS sources.

Figure 16 (from the M4 field discussed in §4.1.3) shows that matching between high precision *HST* observations and ground-based observations can be challenging, especially in crowded regions. In this figure the yellow circles show the HSC objects and the red circles show the

parison for these objects (mainly stars) as a function of magnitude. Breaks in magnitude are employed to make it easier to see how the resulting uncertainties increase for fainter objects, as expected. However, note that there is also a small fraction of objects with unexpectedly large errors. Cutout images show that most of these cases are due to stars with close companions.

The bottom panel shows how the values of the RMS scatter for individual objects grow from about 2 or 3 mas for the brightest objects to about 8 mas for the faintest objects for this particular dataset (i.e., long exposures using ACS/WFC).

We next turn to other measurements in the HSC for the M31 dataset. The upper panel in Figure 15 shows how values of Dsigma from the HSC vary with magnitude. Dsigma is defined as the RMS scatter in the individual measurements for each visit (i.e., D) after all the images have been matched in position (i.e., step 5 discussed in §3). Note that the resulting values of Dsigma are similar to the values of the RMS-X comparison with the Brown et al. (2009) positions from Figure 14, with median values ranging from about 2 to 6 mas as a function of magnitude. The bottom panel shows how the values of Dsigma increase with concentration index (CI), as expected since the objects with large values of CI are generally galaxies

Radio Catalog	# matches[a]	RA offset[b] (arcsec)	Dec offset[b] (arcsec)	Uncertainty[c] (arcsec)
(1)	(2)	(3)	(4)	(5)
FIRST	939	−0.002	0.017	±0.010
VLA COSMOS	469	0.030	−0.074	±0.005
ICRF2	185	0.003	0.013	±0.001

[a] Number of sources matched in the HSC excluding ambiguous matches as described in the text.
[b] Mean position difference (HSC match position–radio position).
[c] Uncertainty in the mean; i.e., the RMS scatter divided by the square root of the number of matches.

PanSTARRS objects. In this particular field more than half of the PanSTARRS objects are clearly blends of several stars when observed with *HST* resolution. However, by restricting the matches to have precisions better than 100 mas, and photometrically similar measurements, we are able to determine good matches for relatively isolated objects (e.g., the blue circles). Using the whole M4 field rather than just this small cutout we find relative accuracies of about 54 mas for single objects, and mean absolute offsets for the ensemble of HSC and PanSTARRS matches in this field of about 9 mas. Hence, the agreement between the HSC and PanSTARRS positions is about a factor of 10 times better than the absolute astrometric accuracy for PanSTARRS (i.e., 100 mas), and hence does not result in much additional degradation to the absolute astrometry for the HSC.

Making the same comparison for a variety of other fields (e.g., sparser and more crowded fields; galaxies with crowding or high background, faint galaxy fields such as the HDF) results in mean offsets between HSC and PanSTARRS positions with values in the range 5 mas (e.g., M87, with isolated, high S/N globular cluster) to 15 mas (M83, with crowding and high background). We conclude that the absolute accuracy for the HSC is essentially the same as for PanSTARRS and 2MASS (i.e., $\sim$0.1 arcsec).

As discussed in §3.1, not all HSC fields can be matched with PanSTARRS, SDSS, or 2MASS. In most cases this is because the PanSTARRS and SDSS surveys do not cover the particular region of the sky, or because the density of 2MASS sources is too low to provide enough matches to make a useful comparison (which is common for Galactic latitude $|b| \gtrsim 20°$). Some *HST* observations have such a large mismatch in wavelength, or have such low quantum efficiency (e.g., far UV observations with WFPC2) that no good matches can be found, especially with the near-IR observations from 2MASS. These cases are defined with the `AbsCorr = N` flag, and have values for absolute astrometry accuracies at the level provided by the HLA (see the HLA FAQ discussion). In many cases, such as early WFPC2 observations, this may be 1 or 2 arc seconds. In a few very rare cases absolute errors up to 10 or 20 arcsec are present, will be discussed in §4.3.3.

4.2.3. *Independent Absolute Astrometric Check using Radio Observations*

The above comparison demonstrates that the HSC is well-aligned to the PanSTARRS coordinate system, as expected since most HSC fields in the sky area covered by PanSTARRS used that catalog to correct the astrometry.

As a completely independent astrometric test, we have also matched the HSC to several different radio catalogs. The astrometric calibration of radio positions relies on a grid of calibration sources. The current International Celestial Reference Frame (ICRF2; Fey, Gordon & Jacobs 2009) has an internal accuracy of better than 1 mas.

We cross-matched three different radio catalogs with the HSC. These catalogs were chosen to provide a broad range of tests of the *HST* astrometry:

- The VLA FIRST survey (Becker et al. 1995; White et al. 1997; Helfand et al. 2015) covers 10,000 deg^2 of the northern sky with a FWHM resolution of 5$''$4 and a source density of $\sim$ 90 sources deg^{-2}. Its major advantage is that it covers a wide sky area (making it more sensitive to large scale systematics), while its disadvantage is a modest resolution that results in RMS accuracies in the radio source positions ranging from 0.1 to 0.5 arcsec depending on brightness.

- The VLA COSMOS survey (Schinnerer et al. 2007) covers the 2 deg^2 COSMOS field with very deep observations (10 times fainter than FIRST) at a FWHM resolution of 1$''$8. Its advantage is that it provides a dense radio catalog (1800 sources deg^{-2}) over a region that also is completely covered by *HST* observations so that there are many HSC-radio matches. Note that it samples only one spot in the sky, however, so it might not be representative of the rest of the HSC.

- The ICRF2 catalog (Fey, Gordon & Jacobs 2009), as mentioned above, is the basic astrometric reference catalog defining the radio coordinate system. It includes 3414 sources spread over the entire sky with extremely accurate radio positions having errors typically less than 1 mas.

For each radio catalog, all HSC sources within 8 arcsec of a radio position were first extracted. The large matching radius was used both to allow for the possibility of a large difference in the HSC and radio positions, and to identify cases where the HSC catalog was too crowded to allow a confident identification of the counterpart. The closest match was accepted as the optical counterpart of the radio source if it was close enough to make the Poisson probability of a chance match P_F less than 0.03:

$$P_F(r, N) = 1 - \exp\left[-N(r/R)^2\right] < 0.03 \quad , \quad (1)$$

where r is the distance to the closest match, and N is the number of matches within search radius $R = 8''$.
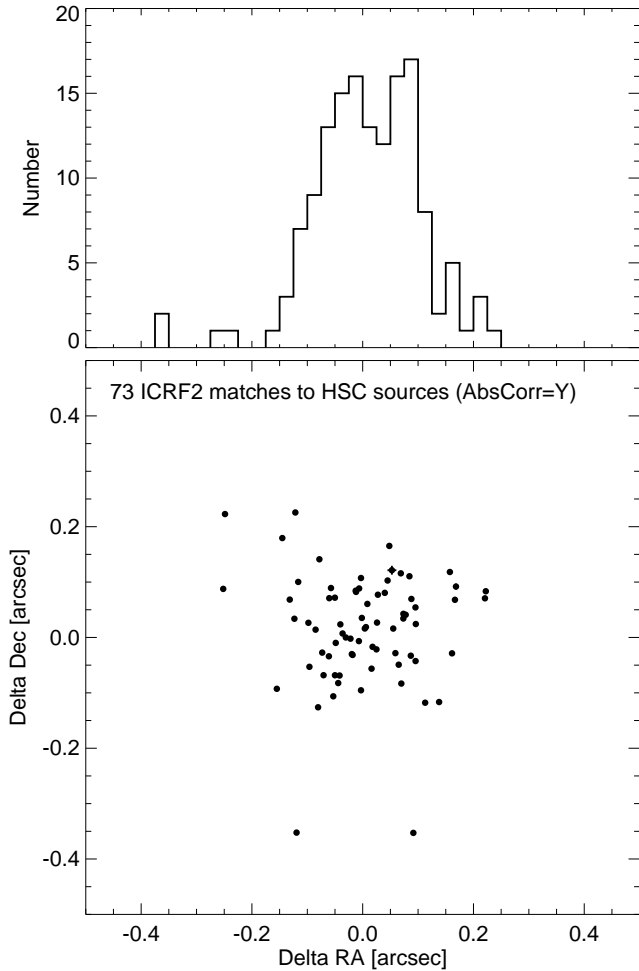
Figure 17. Astrometric comparison of the HSC with the ICRF2 radio astrometric reference catalog (Fey, Gordon & Jacobs 2009). Only HSC objects with corrected astrometry in unconfused regions are included (see text for details). The error bars on the radio positions are shown but are mostly smaller than the symbols. The histogram shows the combined distribution of the one-dimensional offsets in RA and Declination.

Most of the rejected objects are radio sources in the nuclei of galaxies that are resolved by *HST* into a large number of sources. Clearly many of these are real associations and could be used when studying the astrophysics of radio sources, but for the purpose of testing the astrometric accuracy of the HSC they can be dropped. After this cut to eliminate ambiguous matches, the remaining contamination by false (random) matches ranges from 0.2% for the ICRF2 to 0.8% for COSMOS to 1% for FIRST.

Table 2 summarizes the results from these three radio cross-matches. The mean shifts in the wide area FIRST survey are less than 20 mas and are consistent with zero. The COSMOS field does show a significant offset of ~ 80 mas between the HSC and radio positions. That is probably representative of the absolute astrometric accuracy for a small region of the HSC. The last column in the table is the uncertainty in the mean position.

The ICRF2 catalog shows very small mean offsets compared with the HSC. There is however scatter in the positions that is much larger than the uncertainties in the

radio positions (Fig. 17). The RMS scatter is ~ 0.1 arcsec. This could be naively interpreted as being the corresponding uncertainty in the HSC absolute astrometry, and it does in fact represent an upper limit on that uncertainty. However, the reality is more complicated. While the ICRF2 radio sources are very compact objects with positions accurately determined from Very Long Baseline Interferometry, there is no guarantee that the position of the corresponding optical source must match exactly that radio position. The corresponding optical emission is often not coming from the same physical region but may instead be from an associated accretion disk, a dense cluster of stars, or from interstellar gas that is heated and ionized by the energetic source that powers the radio emission. Dust in the galaxy may obscure the nuclear source in the optical and shift its apparent position. Consequently, there is "astrophysical noise" in these positions: perfect measurements of any individual radio source position and its optical counterpart may disagree. This is an extra source of scatter in Figure 17.

The other source of positional scatter for these ICRF2 sources is that some of them are very bright, making the HSC positions uncertain. Visual examination of the 10 objects with the largest separations in Figure 17 reveals that five are extended galaxies (two with dusty disks in the center), two are very bright objects (saturated), two are moderately bright (near saturation), and one has no issues and should have an accurate HSC position.

In summary, matches to external radio catalogs confirm that systematic astrometric errors in the HSC are at most 0.1 arcsec, with significant contributions to the measured scatter from the radio-optical morphological differences (i.e., "astrophysical noise"). There is no evidence for significant mean offsets over thousands of square degrees using the FIRST survey. There is an offset of about 80 mas in comparisons with the COSMOS deep VLA survey; that is likely to be typical of absolute astrometric errors in small regions of the HSC.

4.3. *Photometric and Astrometric Database Comparisons*

Another approach to characterizing the quality of the HSC is to make comparisons using measurements from the entire database, rather than the detailed comparisons discussed in Sections 4.1 and 4.2. These have the advantage of including a much larger fraction of the entire database. Hence the approaches are complementary.

4.3.1. *Photometric Database Comparisons*

Figure 18 shows the Version 1 HSC photometric accuracy based on repeat measurements for the entire database.

The data are separated into different detectors and comparisons are made between pairs of flux estimates measured in the same match (i.e., for the same astronomical object) using the large aperture (i.e., MagAper2) for the same filter. Only stellar sources (based on measurements of the concentration index) are used in this comparison, The x-axis is the flux difference ratio defined as abs(flux1-flux2)/max(flux1,flux2). The y-axis is the number of pairs of sources per bin normalized to unity at a flux difference of zero.
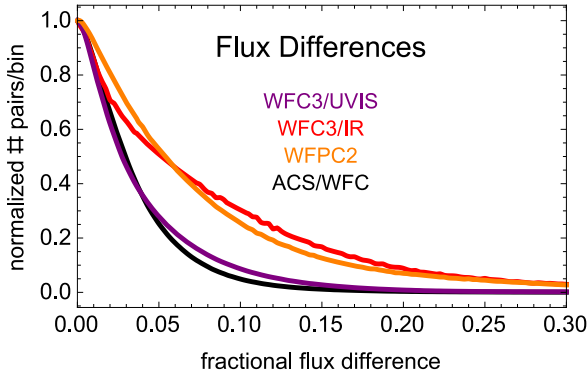
Figure 18. Photometric accuracy for Version 1 of the HSC based on repeat measurements using the entire database.
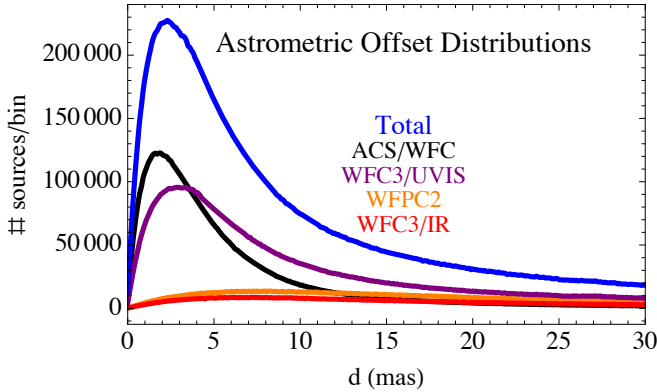

Figure 19. Relative astrometric accuracy for Version 1 of the HSC based on repeat measurements using the entire database.
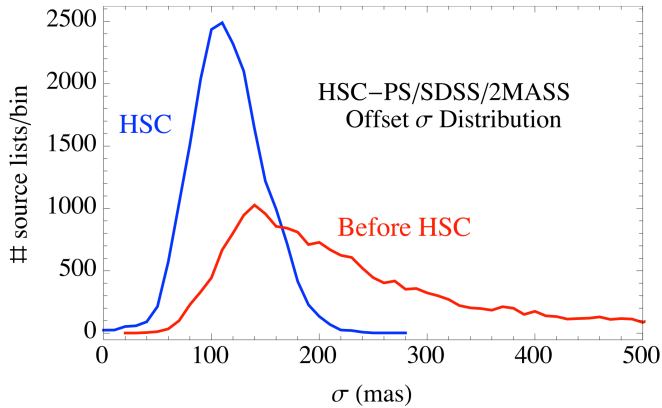
Figure 20. Absolute astrometric accuracy for Version 1 of the HSC based on comparisons with Pan-STARRS, SDSS, or 2MASS. The red line shows the original distribution from the HLA source lists while the blue line shows the distribution after the HSC matching steps have been performed.

4.3.2. Relative Astrometric Database Comparisons

Figure 19 shows a similar comparison for the entire HSC database for the relative astrometry based on repeat measurements, using the white-light detection images. The mode (peak) of the distributions for ACS and WFC3 are roughly 2 mas. The upper curve is the same as the HSC corrected curve in Figure 4. The peak of the distributions for the WFPC2 and WFC3/IR occur at higher values primarily due to the larger pixels (and lower resolutions) for these instruments.
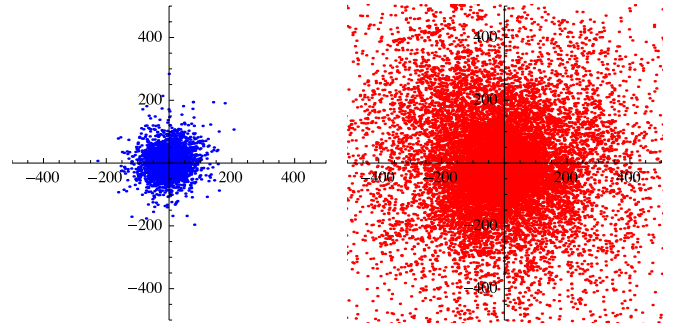
Figure 21. A plot of the mean offsets in source positions with respect to the PanSTARRS, SDSS, and 2MASS catalogs used to determine the match (see §3.1). The horizontal axis is right ascension in mas while the vertical axis is declination in mas. The blue points on the left are for the HSC (i.e., after corrections have been made) while the red points on the right are for the HLA positions.

4.3.3. Absolute Astrometric Database Comparisons

As discussed in §3.1, Step 7 of the HSC pipeline carries out corrections to the absolute astrometry by cross matching with external catalogs (PanSTARRS, SDSS, and 2MASS) where possible. We describe here the accuracy of the absolute astrometry that has been achieved for the HSC relative to these catalogs.

The blue line in Figure 20 shows the resulting absolute astrometry after the HSC matching steps described in §3.1 have been performed. To determine the positional residuals we determine the closest external catalog source within 0.3 arcsec of each HSC match position, using the same external catalog that was used in Step 4 in §3.1 for that source list. The resulting distribution is quite tight, with mean and median values near 120 mas, in general agreement with the results from §4.2.3 based on comparisons with radio observations. The standard deviation is just 34 mas.

The red line in Figure 20 shows the absolute astrometry before the HSC matching steps described in §3.1 have been performed. The resulting distribution is much broader, with a mean value of 450 mas and median value of 220 mas. The large difference between the mean and median values show that there are some very large residuals, in a few rare cases more than 10 arcsec. This is also reflected in the standard deviation, which is 1.1 arcsec for the uncorrected HLA positions.

Figure 21 plots the mean offsets in mas for the right ascension (horizontal axis) and declination (vertical axis). Each plotted point corresponds to a single white-light source list. The left panel (blue) shows the offsets after HSC corrections and the right panel (red) is before HSC corrections. The right panel has a halo that extends well beyond the plotted region. The results show that the uncorrected astrometric offsets have a much broader central core than the corrected ones and also have a long tail. The results also suggest that a mean overall shift is present in the uncorrected *HST* astrometry that is not present after correction. Among source lists with positional shifts less than 300 mas, the mean (RA, Dec) shift is $(-11, -7)$ mas before correction and $(0.01, 0.7)$ mas after correction.

We conclude that the HSC has typical internal photometric accuracies better than 0.1 mag, relative astrometric accuracies of ∼10 mas, and absolute astromet-

ric accuracies of ∼100 mas, although in specific regions the accuracies can be better or worse, due to the inherent non-uniformity of the HSC. These values are in good agreement with the spot checks shown in §4.

4.4. *Incompleteness*

The HSC is incomplete for a number of reasons. For example, only three of the 12 instruments flown on *Hubble* are included; WFPC2, ACS/WFC, and WFC3. However, these are the three instruments with the largest numbers of *Hubble* detections, hence contain the majority of all the sources ever observed by *HST*. Future plans call for the inclusion of NICMOS and ACS/HRC observations, and possibly others in the future (e.g., STIS imaging).

It is also important to remember that even for the three instruments included in Version 1, only about 65% of the ACS/WFC, WFPC2, WFC3 images are included in the catalog due to image quality and other issues (see §3.1 and 4.2.3 for a discussion). In addition, as will be stressed in Section 5, the quality and depth of the source lists for the three instruments is non-uniform. While this will be improved in the future, the HSC will always have different completeness thresholds in different regions for a number of reasons, including the different quantum efficiencies of the instruments (i.e., WFPC2 is much shallower than ACS and WFC3) and the wide range in exposure times.

For these and other reasons, researchers should be aware that just because a source is not in version 1 of the HSC does not mean that there is no *Hubble* observations of it. The HLA can be used to make a more complete search, but for a definitive determination (e.g., when checking for duplications when writing *HST* observing proposals), the MAST archive tools must be used.

5. CAVEATS AND WARNINGS

As stressed in many sections of this paper, the HSC is not a typical wide-area, uniform catalog such as 2MASS, SDSS, or PanSTARRS. It is based on a diverse set of observations using pencil-beam exposures covering only a small fraction of the sky. While it has tremendous potential for doing science, it can also easily be misused. Users should not simply use the HSC as a database search tool. They need to:

- View the HSC overlaid on images. While the vast majority of the source lists are quite good, there are also problem areas that can contain obvious artifacts (e.g., see Figures 22, 23, and 24).

- Try different selection filters (e.g., `NumImages >` some number) to see how it affects the science results. Other potentially useful selection filters are discussed in §4.1.4 . In many cases results from observations using different instruments can also be compared.

5.1. *Five Things You Should Know about Version 1 of the HSC*

New users should keep the following in mind when using the HSC.

1. Detailed use cases and videos are available for training. See Appendix D for pointers.

2. Coverage in certain regions can be very non-uniform (unlike surveys such as SDSS), since source lists have been combined for pointed observations from a wide range of *HST* instruments, filters, and exposure times.

3. WFPC2 and ACS source lists are of poorer quality than WFC3 source lists. As we have gained experience the HLA source lists have improved. For example, many of the earlier limitations (e.g., depth, difficulty finding sources in regions of high background, edge effects, . . .) have been improved in the WFC3 source lists. These improved algorithms will be used when making new WFPC2 and ACS source lists, and will be incorporated into a future release of the HSC.

4. The default is to show all HSC objects in the catalog. This may include a large number of artifacts. You can request `NumImages > 1` (or more) to filter out many artifacts in the HSC. (But in regions covered by only a single *HST* filter, this will remove all HSC sources.)

5. The default is to use aperture magnitudes (i.e., `MagAper2`) in the ABMAG system. Transformations are necessary to convert to other systems (e.g., VEGAMAG or STMAG), or from one instrument to another, or to other photometric systems (e.g., Johnson-Cousins or SDSS ugriz). Transformations are available in a variety of references (e.g., Holtzman et al. 1995 for WFPC2 and Sirianni et al. 2005 for ACS), but for a generic reference stsdas.synphot can be used. Aperture corrections are needed to convert aperture magnitudes to total magnitudes for stars. For extended sources `MagAuto` can be requested.

6. SUMMARY AND FUTURE PLANS

Version 1 of the Hubble Source Catalog includes WFPC2, ACS/WFC and WFC3 photometric measurements based on SExtractor source lists from data release DR8 of the Hubble Legacy Archive. The current version of the catalog includes roughly 80 million detections of 30 million objects involving 112 different detector/filter combinations and about 160 thousand *HST* exposures. The mean photometric accuracy is better than 0.10 mag and the relative astrometric residuals are typically within 10 mas. Better precision (e.g., to 0.02 mag and 2 mas or better) is often possible in certain circumstances (e.g., for bright isolated stars). The absolute astrometric accuracy is better than 0.1 arcsec in most cases.

A number of improvements and enhancements for the HSC are planned for the future. In the relatively short term, the primary improvement will be to upgrade the WFPC2 and ACS source lists using the algorithms developed for the WFC3. We also plan to incorporate HLA
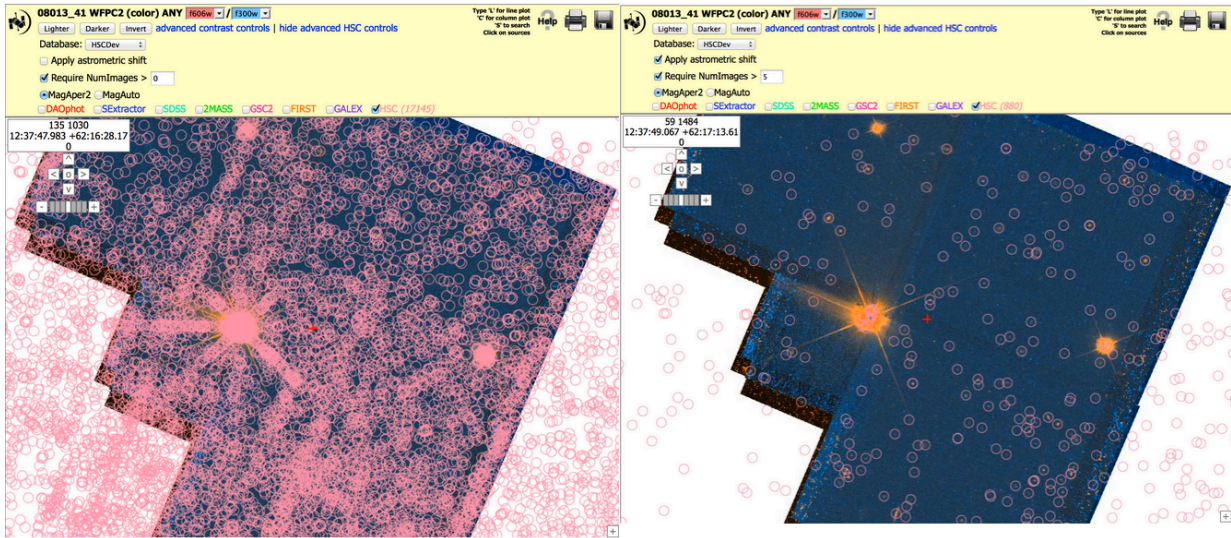
Figure 22. Example of a particularly bad WFPC2 source list (left image) showing artifacts from bright stars and edge effects. The small pink circles are objects in the HSC. Using `NumImages > 5` (right image) removes most of these artifacts.
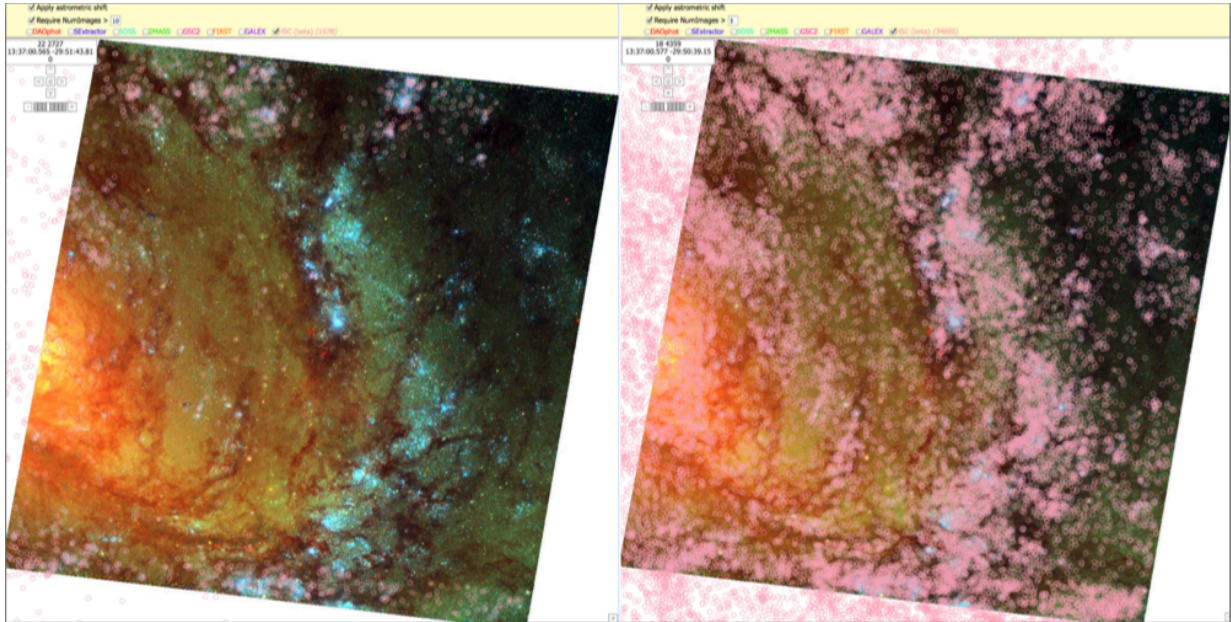
Figure 23. An example of the non-uniformities that are possible using improper search criteria, in this case `NumImages > 10` (left image) rather than > 3 (right image). Additional source lists from overlapping HLA images in the upper and lower parts of the galaxy (M83), images not shown here, result in various corners and linear features in the left image.

source lists for observations taken with the ACS High Resolution Camera (ACS/HRC) and Near Infrared Camera and Multi-Object Spectrometer (NICMOS).

A more fundamental improvement planned for the future is to use the precise offsets determined for the HSC to combine the visit-based images into deeper mosaics. HLA source lists will then be obtained using these images to develop much deeper catalogs (e.g., see Figure 25, where a mosaic image goes roughly four magnitudes deeper). "Forced photometry" at the locations determined from the mosaic images will then be performed for all exposures. This procedure will also provide better information about nondetections and upper limits.

Other planned additions are the incorporation of PSF-fitting photometry using the Anderson et al. (2008) pho-

tometry routines, and integration of spectroscopic information into the HSC.

In the near future, it will be possible to improve the absolute astrometry of Pan-STARRS by linking it to the *Gaia* catalog. Then, by matching the HSC with the improved Pan-STARRS catalog, the resulting absolute astrometric accuracy of the HSC will improve from ~ 0.1 to ~ 0.01 arcsec. One of the motivations for improving the absolute astrometry is to make more reliable identifications of *HST* sources with objects observed by other telescopes at different wavelengths (e.g., X-ray, UV, IR, mm, and radio). Improving the HSC absolute astrometry will ensure that this term of the error budget is negligible compared to the absolute astrometric accuracies of most other telescopes, including *Chandra*, *Spitzer*,
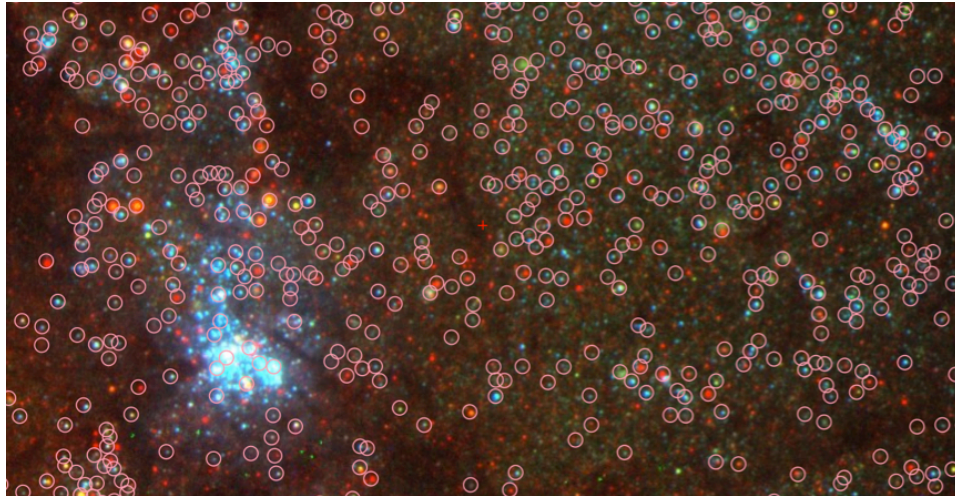
Figure 24. A blowup near the center of the right panel in Figure 23. Note that while the catalog is quite good in general, it is missing some stars in regions of high background.
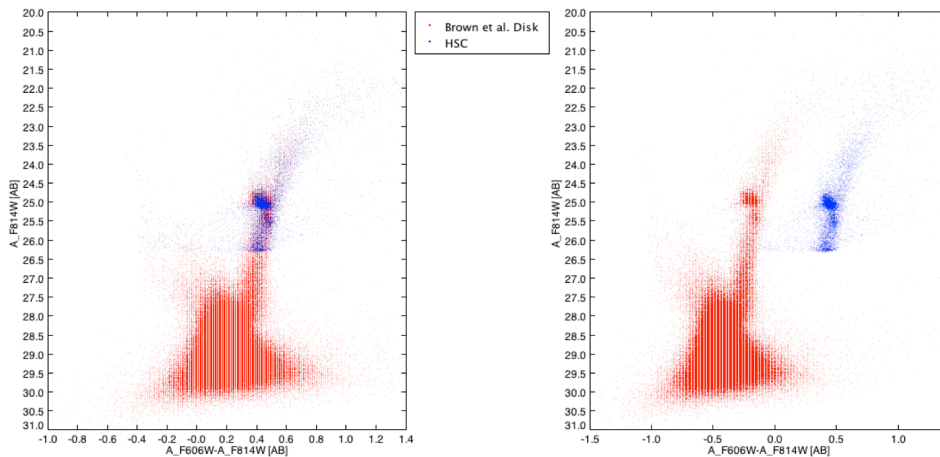
Figure 25. Comparison of HSC photometry (blue) and Brown et. al., (2009) photometry (red). An offset has been added in the right panel to make the comparison of small details easier. See Figures 5 and 6, HSC Use Case #1, and HSC Archival Use Case #1 for more details.

and *GALEX*, and will even provide accuracies comparable with that of mm and radio interferometers such as ALMA and JVLA.

The tools used to access the HSC will also be enhanced in the next few years. One of the primary goals is to better integrate the tools discussed in §5 (the MAST Discovery Portal, the HSC CasJobs service, the HSC home page and the HLA Interactive Display) so that a single interface will allow users easy access to most of the capabilities that are currently distributed across four separate interfaces. Another challenge on the longer term will be to develop tools to more easily combine and compare multiwavelength data sets (e.g., with different spatial resolution) and multi-dimensional data-cubes (e.g., from ALMA and *JWST*).

We encourage the development of value-added-projects based on the HSC database. An example that is already under development is an ESA-based project to develop a Hubble Catalog of Variables (http://www.spacetelescope.org/forscientists/announcements/sci150008/). Other possibilities that are under discussion are the determination of transformation equations to support the combination of data from different instruments, and determinations of photo-Z redshift estimates based on HSC data. We expect that in many cases the products of the value-added projects will be integrated into future version of the HSC.

Catalogs have been a mainstay in astronomy for centuries. Historical examples include the Messier, Herschel and New General Catalogs. More recent examples include 2MASS, *Hipparcos*, and SDSS. In many ways the Hubble Source Catalog will be unique, first and foremost because of the depth and spatial resolution of the *Hubble* image. The HSC will be an important reference for future telescopes, such as the *James Webb Space Telescope*, and survey programs, such as LSST.

In this paper we have attempted to demonstrate the potential of the HSC while also educating HSC users regarding possible pitfalls. The key point is that by its very nature (i.e., deep pencil-beam observations using a wide variety of instruments and observing modes), the HSC is a very different database than most other surveys that have uniform "all-sky" coverage (e.g., SDSS). While the diversity of the HSC dictates the need for caution when developing queries and analyzing data, it also provides the opportunity for cross checking the results in many

cases.

Astronomers will use the HSC in different ways. At the most basic level it provides a quick way to determine what *Hubble* observations have been taken of an object. When building your own catalogs, the HSC can be used as a consistency check. Some people will use the HSC to do feasibility checks, and to perform preliminary analysis. In other cases users will be able to use the catalog to address their primary science goals.

We expect the quality of the HSC to continually improve, as known problems are fixed and new reduction techniques are incorporated. While care will be required in using the Hubble Source Catalog, due to its inher-

ent non-uniformity, it is clear that the HSC provides a powerful new tool for research with *Hubble* data.

APPENDIX

A. COMPARISONS WITH STUDIES BASED ON USE CASES

In this section we examine three specific science projects to see whether using the HSC would give similar results.

A.1. *Brown et al. (2009)—Color Magnitude Diagram in the Outer Disk of M31*

Figure 25 shows a comparison of HSC photometry with the Brown et al. (2009) study of an outer disk region in the Andromeda galaxy. At the brighter magnitudes the comparison is quite good, as discussed in §4.1.1. However, the Brown et al. data is deeper than the HSC by approximately four magnitudes, as expected since this comes from a mosaic where all 30 visits are co-added together compared to the HSC where the measurements are from individual one-orbit visits. However, it should be noted that the photometric uncertainties at these very faint magnitudes are very large, which precludes the use of these stars for much more than counting purposes.

More typically, *Hubble* observers employ just one or two longer visits, hence the difference between the HSC and co-added mosaics is generally much smaller. Nevertheless, HSC users should be aware that it is often possible to go deeper, or to obtain more precise measurements than possible from the general-purpose catalogs produced by the HLA using only the visit-based source lists.

See Figure 6 for a one-to-one comparison of magnitudes for individual sources, and HSC Use Case #1 and HSC Archival Use Case #1 (using the Beta 0.2 version of the HSC) for more detailed discussions.

#### A.2. *Bernard et al. (2010)—Variability in IC 1613*

Figure 26 shows the result of a search of the HSC for variable stars in the dwarf galaxy IC 1613, a field studied in detail by Bernard et al. (2010). In total we find 210 candidate variable stars from the HSC, compared to 259 found in the Bernard et al. (2010) paper. HSC Use Case #3 uses this dataset to show a simple version of how to find variable stars using the HSC, while HSC Archival Use Case #2 shows a detailed treatment using the Beta 0.2 HSC database.

A.3. *Gladders et al. (1998)—The Slope of the Elliptical Red Sequence in Abell 2390*

Figure 27 shows a re-creation using the HSC of the study of the red sequence for elliptical galaxies in Abell 2390 by Gladders et al. (1998). After applying aperture corrections from the *HST* exposure time calculator, as provided in the HSC FAQ, and extinction values from Schlegel et al. (1998), as provided in the HSC Summary Form, the agreement with the slope found by Gladders et al. is quite good (i.e., $m = -0.042 \pm 0.007$ using the HSC and $m = -0.037 \pm 0.004$ from Gladders et al. 1998). See HSC Use Case #6 for a more detailed discussion.
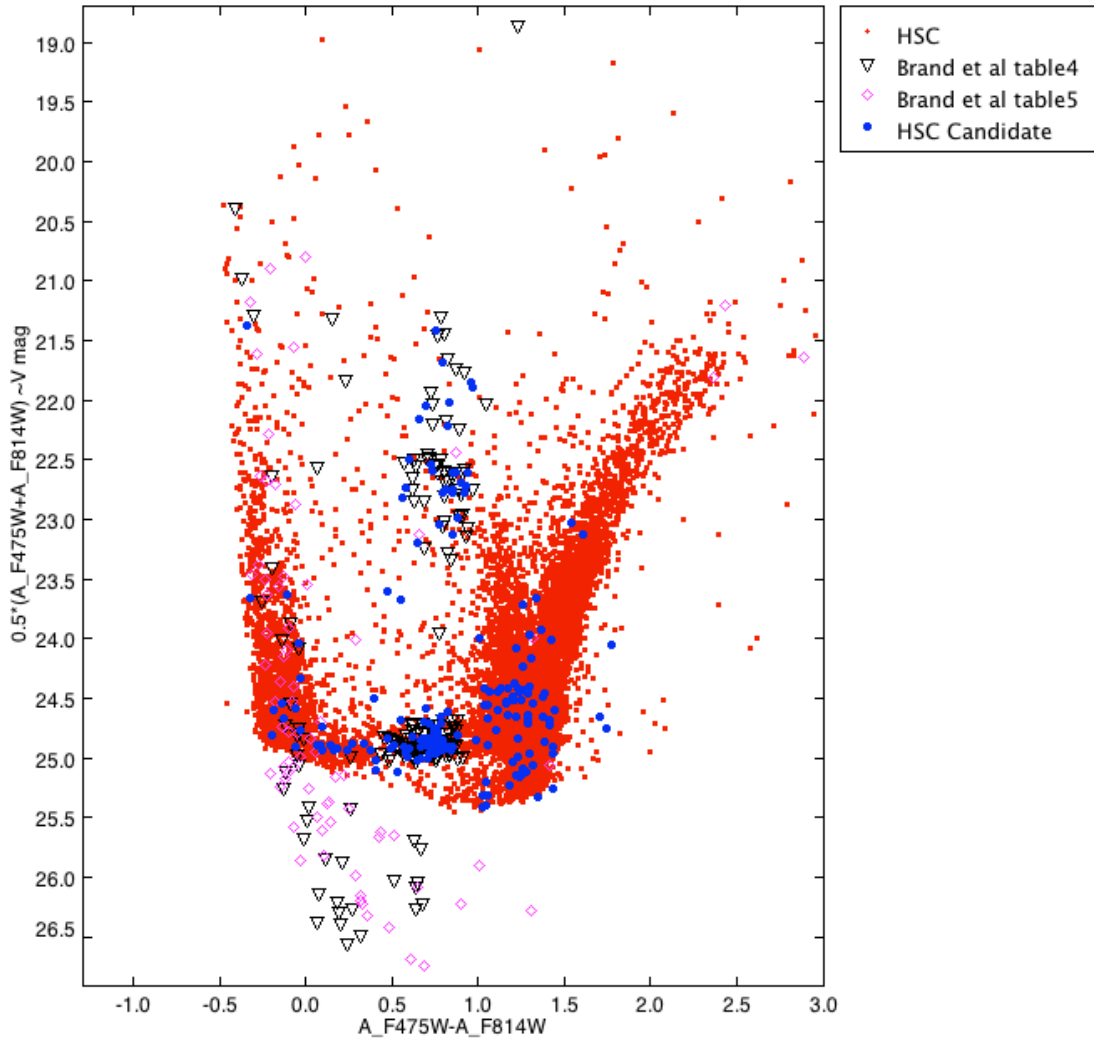
Figure 26. The Color-magnitude diagram for IC 1613. HSC non-variable stars are shown in red while HSC candidate variables are plotted in blue. Variables stars from Bernard et al. (2010) are included (see insert for symbol definitions). The vertical dashed lines roughly delimit the instability strip. Note that the HSC candidate variables are found in the same part of the diagram as the Bernard et al. variables, but do not go as deep. However, the regions of the diagram containing Cepheids and RR Lyrae variables are well covered within the HSC limiting magnitude in this region. See HSC Use Case #3 and archival HSC Use Case #2 for details.
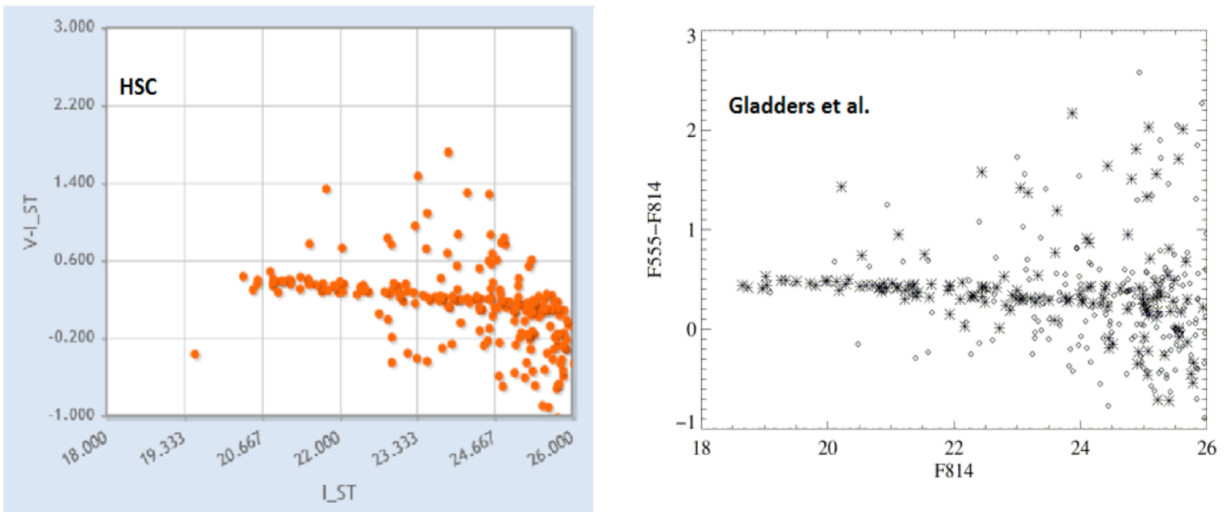
Figure 27. The red sequence for galaxies in Abell 2390 from HSC Use Case #6 (left), showing good agreement with the original Gladders et al. (1998) study (right). The HSC magnitudes are shifted slightly relative to the Gladders et al. plot since the HSC uses ABMAG and Gladders uses STMAG magnitudes, as discussed in more detail in the use case.
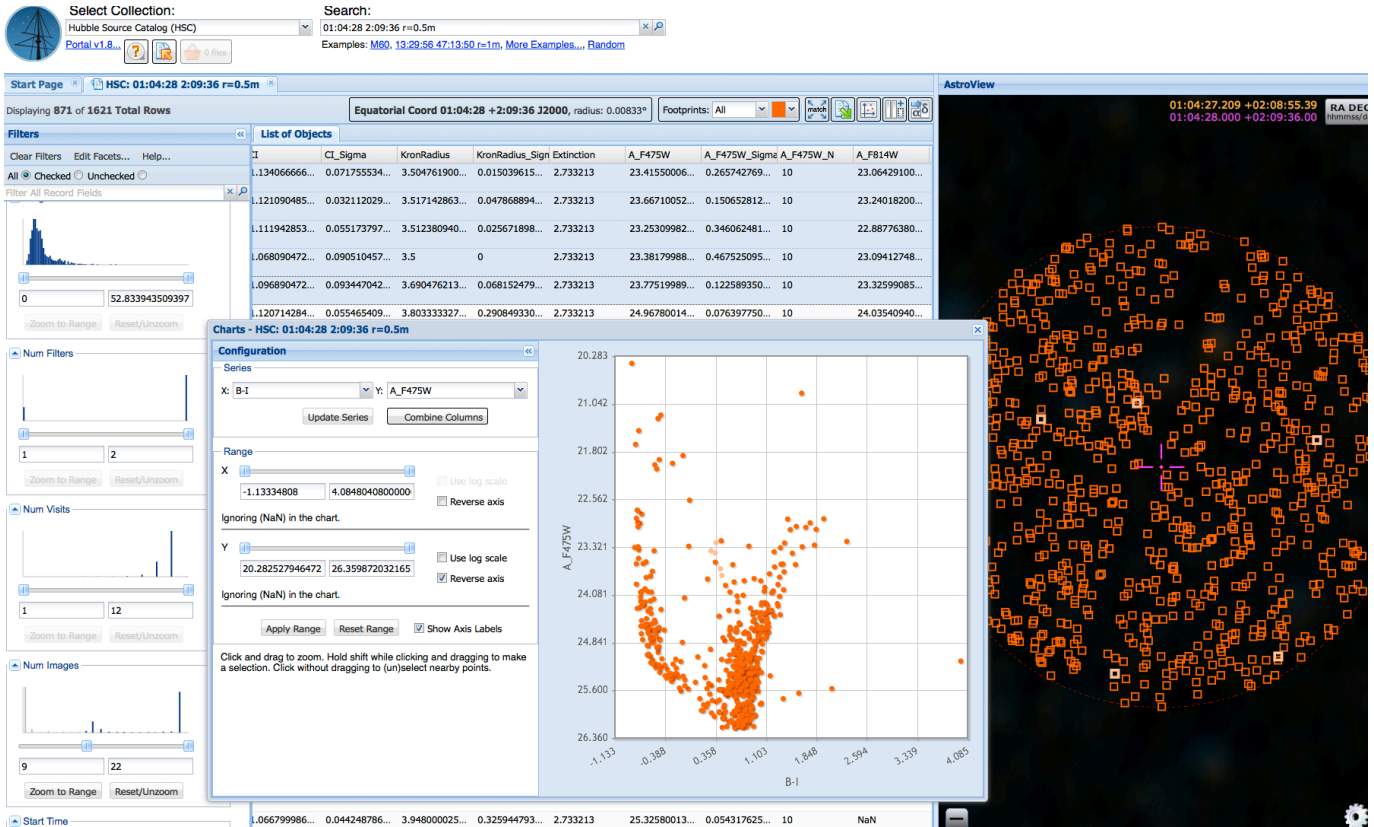
Figure 28. Screenshot from HSC Use Case #3 showing various aspects of the MAST Discovery Portal.

B. TOOLS FOR ACCESSING THE HSC

There are four ways to access Version 1 of the HSC. This is partly due to the historical evolution of the tools, but also reflects the need to provide different types of services, as described below. See Appendix D for a summary of URLs to access the HSC tools and related sites.

B.1. *MAST Discovery Portal (Browsing, Filtering, Plotting, and Cross Matching)*

The primary access tool for the HSC is the MAST Discovery Portal (`http://mast.stsci.edu`). This generally provides the best way to browse what is in the HSC and to do some quick plotting and/or cross matching with other data. It also allows users to download the needed data for further analysis. Its primary current limitation is that only 10,000 sources can be included in a given search, and only `MagAper2` (aperture magnitudes using the larger aperture), rather than `MagAuto` (extended photometry) magnitudes are included. However, as discussed in the next section, CasJobs can be used to obtain larger samples, and/or retrieve values of `MagAuto`. These values can then be filtered and uploaded into the Discovery Portal if desired.

Originally developed as part of the Virtual Observatory initiative, the Portal is now the principal access tool for all MAST data. It has been modified to include access to HSC data and to include features needed to view *HST* images. It includes a wide range of tools for viewing, filtering (e.g., setting a minimum `NumImages` to remove residual cosmic rays and other artifacts), plotting, cross-matching, and downloading.

Figure 28 shows an example of how the Discovery Portal (shown as it appeared for the Version 1 release— modifications can be expected in the future) can be used to find variable stars in IC 1613 (from HSC Use Case #3).

B.2. *CasJobs (Advanced Search and Analysis)*

The Catalog Archive Server Jobs System (CasJobs) was developed by the Johns Hopkins University/Sloan Digital Sky Survey (JHU/SDSS) team. With their permission, MAST has used CasJobs to provide database query access to several MAST databases, including *GALEX*, *Kepler*, and most recently the HSC (`http://mastweb.stsci.edu/hcasjobs`). The purpose of CasJobs is to permit large queries, phrased in the Structured Query Language (SQL), to be run in either real time or in batch queues. Therefore, it does not have the limitations of only including a small subsample of the HSC, as is the case for the MAST Discovery Portal. CasJobs queries may run for hours and may produce large output tables with millions of sources that are stored in the user's MyDB work area. CasJobs is a very powerful interface. However, it is more difficult to learn to use than the Portal and also does not have the wide variety of graphic tools available in the Discovery Portal.

Figure 1 shows an example of how CasJobs can be used to make a color magnitude diagram including 385,675 ACS sources in the Small Magellanic Cloud in less than two minutes (from Use Case #2). Figure 29 shows an example

Figure 29. Example of a HSC CasJobs screen from HSC Use Case #2.

of the query screen for CasJobs, in this case for retrieving a sample of globular clusters in M87 (also from HSC Use Case #2).

B.3. *HSC Home Page (Summary and Detailed Search Forms)*

The HSC Home Page (`http://archive.stsci.edu/hst/hsc`) represents a more basic level of sophistication. This was the original access tool (e.g., for the Beta releases), and while it is useful for certain very detailed searches, it has been largely superseded by the Discovery Portal and HSC CasJobs. It does, however, provide straightforward programmatic access to the HSC with a Virtual Observatory-compatible cone search and other scriptable interfaces to the HSC. It also can be used for larger searches than the portal since it allows the selection of objects using parameters other than position (e.g., magnitudes).

There are two forms-based interfaces to the HSC linked from the Home Page that follow the conventions of MAST. These are the summary search form, which allows users to obtain mean magnitudes and other information with one row per match, and the detailed search form, which includes information about each detection that went into the match. The HSC FAQ is also located at this site, providing the next level of detail beyond this paper.

Figure 30 shows an example of how the HSC Home Page can be used to download data from Brown et al. (2009) observations of the outer disk of M31 (from HSC Use Case #1).

B.4. *HLA Interactive Display (Image Browsing, Source Checking)*

The final way to access the HSC is via the Interactive Display within the HLA (`http://hla.stsci.edu`). An "advanced HSC controls" feature allows the user to set a minimum value for `NumImages` in order to filter out cosmic rays and other artifacts. The HSC summary catalog information for a specific object can be displayed by clicking on the sources in the display. Examples of the Interactive Display are shown in Figures 22 and 23. The Interactive Display can also be accessed through the Discovery Portal.

Figure 30. Example of a search using the HSC Summary Search Form, accessible via the HSC Home Page.

C. EXAMPLE PARAMETER FILES FOR GENERATION OF HLA SOURCE LISTS

```
#=========================
# Sample ACS/WFC sextractor configuration file with specific values
# for filter hst_10188_10_acs_wfc_f435w.

# Default configuration file for SExtractor 2.5.0
# EB 2010-12-20
# Adjusted with suitable defaults for one-orbit depth WFC3-IR images
#=======================

 #------------ Catalog --------------
CATALOG_NAME     hst_10188_10_acs_wfc_f435w_sex.cat
                            # name of the output catalog
CATALOG_TYPE     ASCII_HEAD    # NONE,ASCII,ASCII_HEAD, ASCII_SKYCAT,
                            # ASCII_VOTABLE, FITS_1.0 or FITS_LDAC
PARAMETERS_NAME  snpipe.sexparam  # name of the file containing catalog contents
```

```
#----------- Extraction ------------
DETECT_TYPE        CCD                # CCD (linear) or PHOTO (with gamma correction)
DETECT_MINAREA     5                  # minimum number of pixels above threshold
THRESH_TYPE        RELATIVE           # threshold type: RELATIVE (in sigmas)
                                      # or ABSOLUTE (in ADUs)
DETECT_THRESH      1.4                # <sigmas> or <threshold>,<ZP> in mag.arcsec-2
ANALYSIS_THRESH    4                  # <sigmas> or <threshold>,<ZP> in mag.arcsec-2

FILTER             Y                  # apply filter for detection (Y or N)?
FILTER_NAME        gauss_2.0_5x5.conv   # name of the file containing the filter
FILTER_THRESH                         # Threshold[s] for retina filtering

DEBLEND_NTHRESH    32                 # Number of deblending sub-thresholds
DEBLEND_MINCONT    0.005              # Minimum contrast parameter for deblending

CLEAN              Y                  # Clean spurious detections? (Y or N)?
CLEAN_PARAM        1.0                # Cleaning efficiency

MASK_TYPE          CORRECT            # type of detection MASKing: can be one of
                                      # NONE, BLANK or CORRECT

#-------------WEIGHTing -----------
WEIGHT_TYPE        MAP_RMS            # type of WEIGHTing: NONE, BACKGROUND,
                                      # MAP_RMS, MAP_VAR or MAP_WEIGHT
WEIGHT_IMAGE hst_10188_10_acs_wfc_iv2.fits,hst_10188_10_acs_wfc_f435w_rms.fits
                                      # weight-map filename
WEIGHT_GAIN        N                  # modulate gain (E/ADU) with weights? (Y/N)
WEIGHT_THRESH                         # weight threshold[s] for bad pixels

#------------ FLAGging -------------
FLAG_IMAGE         hst_10188_10_acs_wfc_f435w_msk.fits
                                      # filename for an input FLAG-image
FLAG_TYPE          OR                 # flag pixel combination: OR, AND, MIN, MAX
                                      # or MOST

#----------- Photometry -------------
PHOT_APERTURES     2.0, 6.0           # MAG_APER aperture diameter(s) in pixels
PHOT_AUTOPARAMS    2.5, 3.5           # MAG_AUTO parameters: <Kron_fact>,<min_radius>
PHOT_PETROPARAMS   2.0, 3.5           # MAG_PETRO parameters: <Petrosian_fact>,
                                      # <min_radius>
PHOT_AUTOAPERS     3.0,3.0            # <estimation>,<measurement> minimum apertures
                                      # for MAG_AUTO and MAG_PETRO
PHOT_FLUXFRAC      0.5                # flux fraction[s] used for FLUX_RADIUS

SATUR_LEVEL        60000.0            # level (in ADUs) at which arises saturation

MAG_ZEROPOINT      25.6838624451      # magnitude zero-point
MAG_GAMMA          4.0                # gamma of emulsion (for photographic scans)
GAIN               2192.0             # detector gain in e-/ADU
PIXEL_SCALE        0.05               # size of pixel in arcsec (0=use FITS WCS info)

#-------- Star/Galaxy Separation ----------
SEEING_FWHM        0.076               # stellar FWHM in arcsec
STARNNW_NAME       hla_wfc3.nnw        # Neural-Network_Weight table filename

#---------- Background ------------
BACK_TYPE          AUTO               # AUTO or MANUAL
BACK_VALUE         0.0                # Default background value in MANUAL mode
BACK_SIZE          32                 # Background mesh: <size> or <width>,<height>
BACK_FILTERSIZE    3                  # Background filter: <size> or <width>,<height>

BACKPHOTO_TYPE     LOCAL              # can be GLOBAL or LOCAL
BACKPHOTO_THICK    32                 # thickness of the background LOCAL annulus
BACK_FILTTHRESH    0.0                # Threshold above which the background-
```

```
                              # map filter operates


#---------Check Image ----------
CHECKIMAGE_TYPE BACKGROUND,APERTURES,SEGMENTATION,OBJECTS
                              # can be NONE, BACKGROUND, BACKGROUND_RMS,
                              # MINIBACKGROUND, MINIBACK_RMS, -BACKGROUND,
                              # FILTERED, OBJECTS, -OBJECTS, SEGMENTATION,
                              # or APERTURES
CHECKIMAGE_NAME hst_10188_10_acs_wfc_f435w_BGD_sex.fits,hst_10188_10_acs_wfc_f435w_APR_sex.fits,
hst_10188_10_acs_wfc_f435w_SGM_sex.fits,hst_10188_10_acs_wfc_f435w_OBJ_sex.fits
                              # Filename for the check-image


#----- Memory (change with caution!) ------
MEMORY_OBJSTACK  60000        # number of objects in stack
MEMORY_PIXSTACK  10000000     # number of pixels in stack
MEMORY_BUFSIZE   1024         # number of lines in buffer


#------- ASSOCiation --------
ASSOC_NAME      sky.list      # name of the ASCII file to ASSOCiate
ASSOC_DATA      2,3,4         # columns of the data to replicate (0=all)
ASSOC_PARAMS    2,3,4         # columns of xpos,ypos[,mag]
ASSOC_RADIUS    2.0           # cross-matching radius (pixels)
ASSOC_TYPE      MAG_SUM       # ASSOCiation method: FIRST, NEAREST, MEAN,
                              # MAG_MEAN, SUM, MAG_SUM, MIN or MAX
ASSOCSELEC_TYPE MATCHED       # ASSOC selection type: ALL, MATCHED or -MATCHED


#--------- Miscellaneous ----------
VERBOSE_TYPE    NORMAL        # can be QUIET, NORMAL or FULL
WRITE_XML       N             # Write XML file (Y/N)?
XML_NAME        sex.xml       # Filename for XML output
XSL_URL         file:///usr/local/share/sextractor/sextractor.xsl
                              # Filename for XSL style-sheet
NTHREADS        1             # 1 single thread

FITS_UNSIGNED   N             # Treat FITS integer values as unsigned (Y/N)?
INTERP_MAXXLAG  16            # Max. lag along X for 0-weight interpolation
INTERP_MAXYLAG  16            # Max. lag along Y for 0-weight interpolation
INTERP_TYPE     ALL           # Interpolation type: NONE, VAR_ONLY or ALL

#-----------------------------
```

D. ACCESS TO INFORMATION

The four primary ways to access the HSC are:

- MAST Discovery Portal—http://mast.stsci.edu

- HSC CasJobs—http://mastweb.stsci.edu/hcasjobs

- HSC Home Page and Search Forms—http://archive.stsci.edu/hst/hsc/

- HLA Interactive Display—-http://hla.stsci.edu

Other sources of more detailed information include:

- HSC Use Cases http://archive.stsci.edu/hst/hsc/help/HSC_faq.html#use_case

- HSC FAQ http://archive.stsci.edu/hst/hsc/help/HSC_faq.html

- HLA FAQ http://hla.stsci.edu/hla_faq.html

- Discovery Portal User's Guide http://mast.stsci.edu/portal/Mashup/Clients/Mast/data/html/MastHelp.html

- HSC CasJobs Guide http://mastweb.stsci.edu/hcasjobs/guide.aspx

- Space Telescope Science Institute (STScI) Archive Help Desk: archive@stsci.edu

REFERENCES

Ahn, C. P., et al. 2014, ApJS, 211, 17
Alam, S. J., et al. 2015, ApJS, 219, 12
Anderson, J., et al. 2008, AJ, 135, 2114
Anderson, J., & Bedin, L. R. 2010, PASP, 122, 1035
Becker, R. H., White, R. L., & Helfand, D. J. 1995, ApJ, 450, 559
Bertin, E., & Arnouts, S. 1996, A&AS, 117, 393
Bernard, E. J., Monelli, M., Gallart, C., Aparicio, A., Cassisi, S., Drozdovsky, I., Hidalgo, S. L., Skillman, E. D., & Stetson, P. B. 2010, ApJ, 712, 1259
Brown, T. M., et al. 2006, ApJ, 652, 323
Brown, T. M., et al. 2009, AJ, 184, 152
Budavári, T., & Lubow, S. H. 2012, ApJ, 761, 188
Budavári, T., & Szalay, A. S. 2008, ApJ, 679, 301
Dolphin, A. E. 2009, PASP, 121, 655
Fey, A. L, Gordon, D., & Jacobs, C. S. 2009, IERS Technical Note 35:29
Fruchter, A., et al. 2009, *HST* MultiDrizzle, *HST* Data Handbooks,
Gladders, M. D., Lopez-Cruz, O., Yee, H. K. C., & Kosama, T. 1998, ApJ, 501, 571
Helfand, D. J., White, R. L., & Becker, R. H. 2015, ApJ, 801, 26
Holtzman, J. A., et al. 1995, PASP, 107, 1065
Jenkner, H., et al. 2006, ASPC, 351, 406
Lubow, S., & Budavári, T. 2013, Astronomical Data Analysis Software and Systems XXII, 475, 203
Pier, J., et al. 2003, AJ, 125, 1559
Schlegel, D. J., Finkbeiner, D. P., & Davis, M. 1998, ApJ, 500, 525
Schinnerer, E., Smolčić, V., Carilli, C. L., et al. 2007, ApJS, 172, 46
Sirianni, M., et al. 2005, PASP, 117, 1049
Skrutskie, M. F., et al. 2006, AJ, 131, 1163
Stetson, P. B. 1987, PASP, 99, 191
Stubbs, C. W., Doherty, P., Cramer, C., Narayan, G., Brown, Y. J., Lykke, K. R., Woodward, J. T., & Tonry, J. L. 2010, ApJS, 191, 376
White, R. L., Becker, R. H., Helfand, D. J., & Gregg, M. D. 1997, ApJ, 475, 479
Whitmore, B., Lindsay, K., & Stankiewicz, M. 2008, Astronomical Data Analysis Software and Systems XVII, 394, 481
Williams, B. F., et al. 2014, ApJS, 215, 9